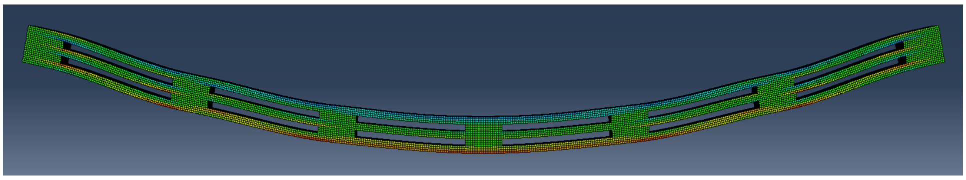

GAP CLT

A study of modelling approaches and material savings

ANTON KRISTENSEN LINDBERG

Structural Mechanics

Master's Dissertation

DEPARTMENT OF CONSTRUCTION SCIENCES
DIVISION OF STRUCTURAL MECHANICS

ISRN LUTVDG/TVSM--26/5284--SE (1-63) | ISSN 0281-6679
MASTER'S DISSERTATION

GAP CLT

A study of modelling approaches and material savings

ANTON KRISTENSEN LINDBERG

Supervisor: Professor **ERIK SERRANO**, Division of Structural Mechanics, LTH.
Assistant Supervisor: **ELIF APPAVURAVTHER**, Postdoc, Division of Structural Mechanics, LTH.
Examiner: **HENRIK DANIELSSON**, Associate Professor, Division of Structural Mechanics, LTH.

Printed by V-husets tryckeri LTH, Lund, Sweden, June 2026 *(Pl)*.

For information, address:
Division of Structural Mechanics,
Faculty of Engineering LTH, Lund University, Box 118, SE-221 00 Lund, Sweden.
Homepage: www.byggmek.lth.se

Abstract

Cross laminated timber (CLT) is a sustainable alternative to concrete in multi-storey buldings. This project examines "Gap CLT", a modified version in which certain lamellas are removed to reduce material use. The reduction of material usage would decrease the CO2 emissions and therefore contribute to the prevention of global warming. However, the structural behavior of Gap CLT is not yet fully understood. For a one way spanning plate, it would be very suitable to remove some of the transverse lamellas as it would theoretically be a good way to save material without drastically affecting the structural capacity in the span direction.

The project aims to evalute the Gap CLT and to assess different design methods in ultimate limit state and serviceability limit state. Analytical methods such as, the gamma method, Timoshenko theory and the shear analogy method are used along with finite element models in FEM-design and Abaqus. By introducing a reduction factor, reduced stiffness parameters are used to represent the gaps. Results from the analytical and numerical methods are compared to identify the possibilities and limitations of Gap CLT, supporting its development as a more efficient and sustainable structural solution.

For the examined design case, a CLT plate with a width of 2 meters and a length of 5 meters is studied. Along with a variable load of 2.0 kN/m^2, a permanent load of 1.5 kN/m^2 and the self weight is considered. It was shown that frequency of the CLT plate was the governing design check. According to the analytical methods, a material saving of 21 % could be achieved for optimized configurations. However, the methods utilizing the reduction factor could not correctly take gaps into account, as shown by the 3D finite element models in Abaqus and FEM-design, which are assumed to give the most realistic results. For these methods, the effect of the gaps was underestimated in serviceability limit state. For the ultimate limit state, only Abaqus managed to take the gaps into account. According to FE-analysis with Abaqus, a material saving of 10 % could be achieved for the examined design case.

Sammanfattning

Korslimmat trä (CLT) är ett hållbart alternativ till betong i flervåningshus. Detta projekt undersöker ”Gap CLT”, en modifierad version där vissa lameller avlägsnas för att minska materialanvändningen. En minskad materialanvändning skulle minska koldioxidutsläppen och därmed bidra till att förebygga global uppvärmning. Gap CLT:s strukturella beteende är dock ännu inte helt känt. För en platta med enkelriktad spännvidd skulle det vara mycket lämpligt att ta bort några av de tvärgående lamellerna, eftersom det teoretiskt sett skulle vara ett bra sätt att spara material utan att drastiskt påverka den strukturella kapaciteten i spännviddsriktningen.

Projektet syftar till att utvärdera Gap CLT och att bedöma olika modellerings metoder i brottgränstillståndet och bruksgränstillståndet. Analytiska metoder såsom gammametoden, Timoshenko-teorin och skjuvanalogimetoden används tillsammans med finita elementmodeller i FEM-design och Abaqus. Genom att införa en reduktionsfaktor används reducerade styvhetsparametrar för att representera hålen. Resultaten från de analytiska och numeriska metoderna jämförs för att identifiera möjligheterna och begränsningarna hos Gap CLT, vilket stödjer dess utveckling som en mer effektiv och hållbar konstruktionslösning.

För det undersökta beräkningsfallet studeras en CLT-platta med en bredd på 2 meter och en längd på 5 meter. Utöver en variabel belastning på 2,0 kN/m^2 beaktas även en permanent belastning på 1,5 kN/m^2 samt egenvikten är beaktad. Det visade sig att CLT-plattans frekvens utgjorde den avgörande beräkningsgränsen. Enligt de analytiska metoderna kunde en materialbesparing på 21 % uppnås för optimerade konfigurationer. Metoderna som använde reduktionsfaktorn kunde dock inte korrekt ta hänsyn till hålen, vilket framgår av de 3D finita elementmodellerna i Abaqus och FEM-design, vilka antas ge de mest realistiska resultaten. För dessa metoder underskattades effekten av hålen i bruksgränstillståndet. När det gäller brottgränstillståndet var det däremot endast Abaqus som lyckades beakta hålen. Enligt FE-analysen med Abaqus kunde en materialbesparing på 10 % uppnås för det undersökta konstruktionsfallet.

Acknowledgements

I would like to express my deepest gratitude to my supervisor Erik Serrano, co-supervisor Elif Appavuravther and examiner Henrik Danielsson for the knowledge, patience and support they have given me throughout the project.

Furthermore, I would also like to express my gratitude towards Jacob Ettrup Pedersen, Sidsel Juhlin and Gustav Scholz at Artelia DK for the collaboration opportunity. As well as the commitment and knowledge they have provided me with during the duration of the thesis.

Anton Kristensen Lindberg, Lund, June 2026.

List of Figures

List of Tables

Notations and Symbols

Latin letters

$f_{m,k}$ - Characteristic bending strength
$f_{t,0,k}$ - Characteristic tensile strength, parallel to grain
$f_{t,90,k}$ - Characteristic tensile strength, perpendicular to grain
$f_{c,0,k}$ - Characteristic compression strength, parallel to grain
$f_{c,90,k}$ - Characteristic compression strength, perpendicular to grain
$f_{v,k}$ - Characteristic longitudinal shear strength
$f_{r,k}$ - Characteristic rolling shear strength
$E_{0,mean}$ - Mean modulus of elasticity, parallel
$E_{90,mean}$ - Mean modulus of elasticity, perpendicular
$G_{0,mean}$ - Mean shear modulus, parallel
$G_{R,mean}$ - Mean shear modulus, rolling shear
k_{sys} - System factor
k_{mod} - Modification factor
k_{def} - Deformation factor
f_d - Design strength
$f_{m,d}$ - Design bending strength
$f_{t,0,d}$ - Design tensile strength, parallel to grain
$f_{t,90,d}$ - Design tensile strength, perpendicular to grain
$f_{c,0,d}$ - Design compression strength, parallel to grain
$f_{c,90,d}$ - Design compression strength, perpendicular to grain
$D_{EI_{eff}}$ - Bending stiffness, gamma method
$I_{ef,x}$ - Effective moment of inertia in the x-direction, gamma method
$I_{ef,y}$ - Effective moment of inertia in the y-direction, gamma method
t_i - Thickness of a specific layer
L - Length of the CLT plate
a_i - Distance from midpoint of the i-layer to the center of gravity, gamma method
D_{EI} - Bending stiffness, Timoshenko theory
D_{GA} - Shear stiffness, Timoshenko theory
I_{net} - Area moment of inertia, Timoshenko theory
e_i - Distance from midpoint of the i-layer to the center of gravity, timochenko theory
$(EI)_{eff}$ - Effective bending stiffness, shear analogy method
$(GA)_{eff}$ - Effective shear stiffness, shear analogy method
z_i - Distance from midpoint of the i-layer to the center of gravity, shear analogy method
b - width of the CLT plate
D_{ii} - Stiffness parameter in stiffness matrix
m_x - Bending in x-direction
m_y - Bending in y-direction
m_{xy} - Torsion around x-direction
v_{xz} - Out of plane shear in xz-plane
v_{yz} - Out of plane shear in yz-plane

n_x - Axial force in x-direction
n_y - Axial force in y direction
n_{xy} - In plane shear in xy-plane
K_x - Curvature displacement due to bending in x-direction
K_y - Curvature displacement due to bending in y-direction
K_{xy} - Curvature displacement due to torsion around x-direction
u - Translation
q_d - Design load
$m_{x,d}$ - Maximum bending moment
$W_{x,net}$ - Section modulus
z_{max} - Maximum distance from midpoint of cross section to one of the edges
$v_{xz,d}$ - Maximum shear force
S_x - Static moment for longitudinal layer
$S_{x,r}$ - Static moment for cross layer
w_{fin} - Final deflection
w_{inst} - Instantaneous deflection
w_{creep} - Deflection due to long term effects
q_k - Characteristic load
$w_{inst,lim}$ - Instantaneous deflection limit
$w_{fin,lim}$ - Final deflection limit
f_1 - First eigenfrequency
I_{mod} - Modal impulse from footsteps
$v_{1,peak}$ - Maximum velocity
m - Surface distributed mass
$v_{tot,peak}$ - Total velocity factor
k_{imp} - Velocity factor
v_{rms} - Final velocity response
w_{1kN} - Deflection due to point load
B_{ef} - Effective width
w_{lim} - Deflection limit due to point load
$g_{k,1}$ - Permanent load
$g_{k,2}$ - Load due to self weigth
L_{RVE} - Length of the RVE-model
B_{RVE} - Width of the RVE-model

Greek letters

ρ_m - Density
γ_m - Partial factor
ψ - Load reduction
γ_d - Safety class factor
Ω - Reduction factor due to gaps
γ_i - Gamma factor for a specific layer
π - Mathematical constant, ratio of circle's circumference to its diameter.
κ - Shear correction factor
γ_{xz} - Shear strain due to out of plane shear in xz-plane
γ_{yz} - Shear strain due to out of plane shear in yz-plane
γ_{xy} - Shear strain due to in plane shear in xy-plane
ϵ_x - Strain due to axial force in x-direction
ϵ_y - Strain due to axial force in y-direction
ϕ - Rotation
$\sigma_{m_x,d}$ - Design bending stresses
$\tau_{xz,d}$ - Design longitudinal shear stresses
$\tau_{xz,r,d}$ - Design rolling shear stresses
ζ - Modal damping factor
η - Factor for velocity response
ς - Reduction factor for displacement on RVE models

Contents

1 Introduction

1.1 Background

Cross laminated timber (CLT) is a prefabricated engineered wood product, consisting of various layers of timber lamellas which are stacked and glued upon each other crosswise. A common use for cross laminated timber is to act as a slab in a floor system, offering a more sustainable alternative to a concrete slab in a multi story building.

In the ongoing research project ”InnoTLT”, a modified version of a cross laminated timber slab is being studied. This version removes either transverse or longitudinal members of the lamellas in order to reduce material usage. However the effect of removing these lamellas in real life use is still relatively unknown. Therefore, the possibilities and the limitations of this “gap CLT” needs to be studied further.

When modelling traditional cross laminated timber, beam theory or plate theory is commonly applied. However, these beam and plate theory models do not always describe the slab with sufficient accuracy. Along with the gaps created by the removed lamellas, the mechanical behavior of the ”gap CLT” is hard to predict with the current approaches. To predict the strength and stiffness of the panels, understanding the behavior plays an important role. The approaches most commonly used are the shear analogy method, Timoshenko theory and the gamma method, which all relate to beam modeling.

1.2 Purpose and aim

The purpose of this thesis project is to contribute to a greater understanding of the structural behavior of optimized cross laminated timber (CLT), also known as ”Gap CLT”, while simultaneously helping the future development of the product, making it more environmentally and economically sustainable by reducing the material usage.

While the aim of the thesis project is to better understand what the possibilities and the limitations of this optimized product is, the project also aims to give further knowledge about what methods are the most suitable in design. Comparing analytical 1D modeling methods such as the Gamma method to 3D finite element models is therefore also included. The importance of this comparison is increasing the knowledge of this optimized product and facilitate future reliable modeling methods. I.e. could the current analytical methods be improved and how suitable would a method using homogenization be.

1.3 Method

The method of completing this project is to compare a design case for 1D modeling methods such as the gamma method, Timoshenko method and the shear analogy method by calculations in the ultimate limit state and the serviceability limit state. These calculations are performed in Excel. To take the gaps into account in the design, the relevant stiffness parameters are adjusted to a lower value, representing the lowered stiffness due to material removed in the direction in question.

The results from the analytical models are then further compared with results of finite element models created in two different FE-software, Abaqus and FEM-design respectively. As for one of the two methods used in FEM-design, a homogenization will be performed through the usage of Abaqus to get a representative stiffness matrix to represent the "Gap CLT".

1.4 Limitations

The main goal of this project is to analyze the structural performance of the "Gap CLT". To fully understand the performance of the product, this project is suggestively need to be complemented by analysis with regard to fire safety, acoustic performance and moisture safety.

Furthermore, calculations in this project are done in regard to Swedish standards. As certain factors and regulations can vary between different countries, the results will therefore also differ.

As some of the design checks in the serviceability limit state, such as point load criterion and velocity response, had a low utilization rate for the analytical methods, they were not further analyzed by the finite element methods.

Finally, the design case examined in this project only examines static loading on a one way spanning 5 layer CLT plate.

2 CLT as a material

2.1 The properties of CLT

2.1.1 Material orientation

Due to the structural composition of timber as an orthotropic material, the properties vary depending on the direction of the material. For a single lamella of a CLT plate, the directions are defined as shown in figure 2.1, with the directions being longitudinal direction, tangential direction and radial direction. In reality, the directions vary within a lamella of a CLT plate and will have great variation between lamellas [1].

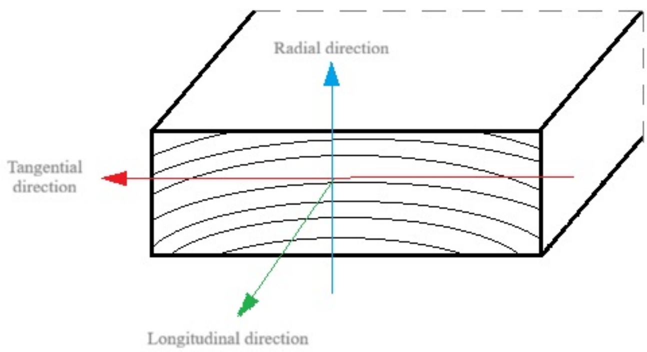

Figure 2.1: Material directions of a timber lamella [2]

Applying the material directions according to figure 2.1 into a (x,y,z) coordinate system for the entire CLT plate, gives the direction definitions as shown in figure 2.2 Here, x is the strong direction and y is the weak direction of the CLT plate.

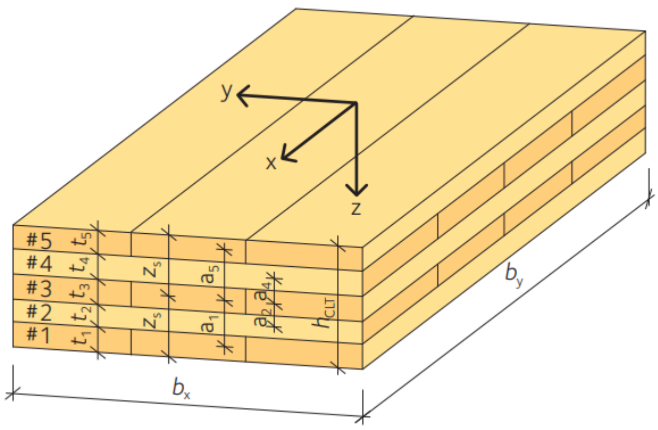

Figure 2.2: Definition of coordinate system for a CLT plate [3]

The cross layup structure of the CLT provides the need for further definition of the material orientation, for instance, in regard to where the longitudinal direction is for a specific layer. Therefore, defining the longitudinal layer direction is done by the annotation of 0, and 90 for the cross layer direction.

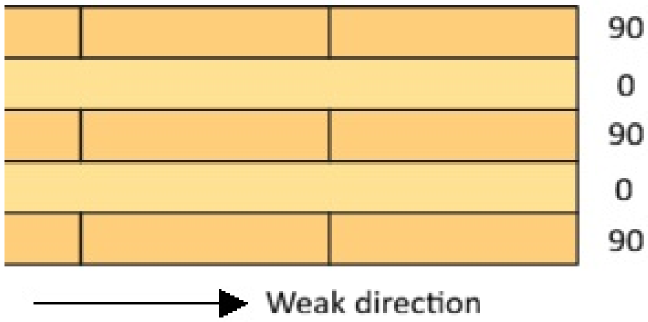

Figure 2.3: Definition of directions for a CLT cross section

2.1.2 Characteristic strength

The characteristic strength values and characteristic stiffness values for CLT panels, which are based on the strength properties of C24 timber boards, are displayed in table 2.1 and table 2.2 respectively. Furthermore, the mean density of the timber boards, denoted ρ_m, is set to 420 kg/m^3 [3].

Table 2.1: Characteristic strength for CLT made from C24 lamellas [3].

Property	Symbol	Characteristic value
Bending strength	$f_{m,k}$	24 MPa
Tensile strength, parallel to grain	$f_{t,0,k}$	14 MPa
Tensile strength, perpendicular to grain	$f_{t,90,k}$	0.4 MPa
Compressive strength, parallel to grain	$f_{c,0,k}$	21 MPa
Compressive strength, perpendicular to grain	$f_{c,90,k}$	2.5 MPa
Longitudinal shear	$f_{v,k}$	4 MPa
Rolling shear	$f_{r,k}$	0.7 MPa

2.1.3 Stiffness values

Table 2.2: Stiffness values for CLT made from C24 lamellas [3].

Stiffness property	Symbol	Value
Mean modulus of elasticity, parallel	$E_{0,mean}$	11000 MPa
Mean modulus of elasticity, perpendicular	$E_{90,mean}$	370 MPa
Mean shear modulus, parallel	$G_{0,mean}$	690 MPa
Mean shear modulus, rolling shear	$G_{R,mean}$	50 MPa

2.2 Basis of design

2.2.1 Partial coefficient and modification factors

Partial factor, γ_m

The partial factor is different for different countries, as the value varies depending on the level of control in design and for manufacturing in the specific country. In Sweden, the factor is given as [3]:

$$\gamma_M = 1.25$$

System factor, k_{sys}

For the multiple lamellas acting together in a CLT plate, Eurocode 5 allows the possibility of increasing the capacity by the factor k_{sys} [1].

The increase of capacity is made able by the composition of CLT, in comparison to regular structural timber, which has a higher probability of a knot affecting the material strength [3].

It usually varies from 0.9 to 1.2, but could also be determined by the following formula:

$$k_{sys} = min(1.15, 1 + 0.1 \cdot b) \tag{2.1}$$

In this work it is set to be:

$$k_{sys} = 1$$

Modification factor, k_{mod}

The selection of the modification factor is dependent on the load duration and a service class. The service class is determined given how much moisture the CLT will be exposed to, where a higher service class, indicates a higher exposure to moisture. The value of the modification factor is chosen to be medium-term load in service class 1 [3]:

$$k_{mod} = 0.8$$

Load reduction, ψ

The use of the load reduction factors are applied depending on whether the variable load is the dominant load or not and the values themselves vary for different loading categories. In this project, the residential category is assumed, which gives the loading factors [4]:

$$\psi_0 = 0.7,\ \psi_1 = 0.5 \text{ and } \psi_2 = 0.3$$

Safety-class factor, γ_d

A factor used in determining the design load, dependent on a safety class. The higher the safety class the higher the risk for injuries to human in regards to failure. As the CLT plate most likely would be part of a multi-story flooring system, the highest saftey class is chosen. Henceforth, the partial coefficient has the value shown below: [4]:

$$\gamma_d = 1$$

Deformation factor, k_{def}

Another factor which is dependent on climate class. This factor affects the creep deformation. However, it is also dependent on the number of layers in the CLT, according to the 5 layer setup and climate class, the value is [5]:

$$k_{def} = 0.8$$

2.2.2 Design strength

For design in the ultimate limit state, the design value of a strength property is needed. It is calculated by applying the partial coefficient and the relevant factors from subsection 2.2.1, according to the formula [3]:

$$f_d = k_{sys} \cdot k_{mod} \cdot \frac{f_k}{\gamma_M} \tag{2.2}$$

Table 2.3: Calculated design strength for CLT made from C24 lamellas.

Property	Symbol	Design value
Bending strength	$f_{m,d}$	15.36 MPa
Tensile strength, parallel to grain	$f_{t,0,d}$	9.28 MPa
Tensile strength, perpendicular to grain	$f_{t,0,d}$	0.256 MPa
Compressive strength, parallel to grain	$f_{c,0,d}$	13.44 MPa
Compressive strength, perpendicular to grain	$f_{c,0,d}$	1.6 MPa
Longitudinal shear	$f_{v,d}$	2.24 MPa
Rolling shear	$f_{r,d}$	0.448 MPa

2.3 Gap CLT

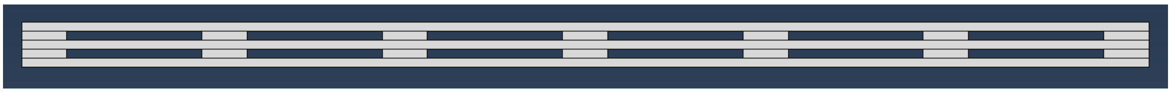

Figure 2.4: Visualization of a CLT plate with gaps

With the introduction of gaps in the CLT plate, the structural behavior will change and the stiffness will be reduced. For the usage of Abaqus when designing in the ultimate limit state and the serviceability state, the effect of the gaps will be taken into consideration in the model itself. In FEM-design, the gaps can be accounted for by creating a stiffness matrix calculated from FE-models in Abaqus, this will be expanded on in later chapter.

However, when using the 1D modeling methods, the gaps need to be represented in another way than in 3D finite element analysis. It is assumed that the best way to represent the gaps is by introducing reduction factors, to adjust the relevant parameters in design. More specifically, the stiffness parameters. The parameters that are to be adjusted, would vary depending on the direction of the gaps.

For a CLT plate, the reduction of the bending stiffness due to gaps is handled according to conclusions made by Franzoni and his colleagues [6]. In their research, they concluded that the bending stiffness is reduced proportionally to the reduction of the material volume for a specific layer. However, it was also concluded that this approach is not adequate for the reduction of the shear stiffness. Therefore, it is suggested that other approaches are used.

Furthermore, Moberg and Xiao [7] concluded that for a CLT plate where transverse lamellas have been removed, configurations with centered air gaps perform better than configurations with shifted air gaps. For visual reference of the placement of the gaps, see figure 2.5.

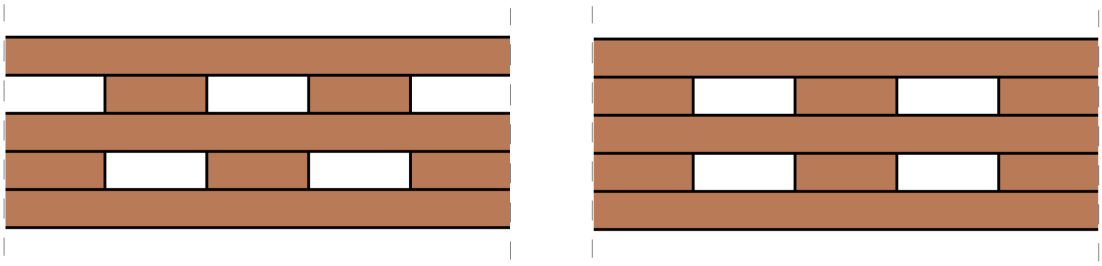

Figure 2.5: Visualization of shifted air gaps (left) and centered air gaps (right) in the transverse layer for a 5 layer CLT plate

As no design basis exists for how the gaps should be taken into consideration, it is decided that the previously mentioned geometrical approach will have to be used for the analytical methods, even though it is not adequate for the reduction of the shear stiffness. However, a more adequate approach could be possible through the usage of FE-analysis. But it is decided that the geometrical approach would be more methodically correct for the analytical methods.

For gaps in the transverse layer, the assumed affected parameters would be the following:

- Longitudinal modulus of elasticity, for the y-direction, $E_{0,y}$
- Modulus of Shear, for the y-direction, $G_{0,y}$
- Modulus of Rolling shear, for the x-direction, $G_{r,x}$

The stiffness values can be found in table 2.2.

Applying the stiffness reductions on the stiffness parameters is only relevant for the serviceability limit state. However, for the ultimate limit state, the reduction also needs to be applied such that the geometry due to the gaps is respected. Although, this would only affect the result for the weak direction for the conventional formulas.

2.3.1 Reduction factor, Ω

To reduce bending and shear stiffness due to the introduction of gaps, a reduction factor is introduced, denoted Ω. The factor represents the ratio of wood volume in a layer with gaps, relative the volume in that layer without gaps. The reason for simply referring to that layer in the CLT is due to the heterogeneous structure of the material. The stiffness reduction factor will be determined according to:

$$\Omega = \frac{V_{material}}{V_{material} + V_{gaps}} \tag{2.3}$$

I.e. for a layer with 40 percent air and 60 percent wood, the value of the stiffness parameter in that layer would then be reduced by 40 percent, since in this case to the factor $\Omega = 0.6$.

3 CLT modelling

3.1 1D – Beam

When modeling CLT in 1D, there are three major modeling methods that are usually used. Calculations according to the conventional Bernoulli-Euler beam theory is not applicable for CLT due to the structural composition of the material. The crosswise layup of the timber lamellas results in the occurrence of both longitudinal and rolling shear stresses when loaded perpendicular to the plane. As the stiffness in regards to rolling shear is low, the shear deformation must be considered. While Bernoulli-Euler theory only considers the bending deformation, the Gamma method, Timoshenko theory and Shear analogy method takes the shear deformation into account as well, therefore being necessary to implement when modeling [3].

3.1.1 Gamma method

For CLT, the gamma method is a means to take the shear deformation into account by the usage of a so called effective bending stiffness, $D_{EI,ef}$. It consists of the stiffness parameter, E and an effective moment of inertia, I_{ef}, where a gamma-factor, γ, is introduced to calculate the effective moment of inertia [5].

The principle of introducing the gamma-factor is to reduce the stiffness parameter with regard to the interaction between the layers. The value can range from 1 to 0, where a higher value indicates high connection efficiency, while a lower value indicates a lower composite action. A limitation to this method is that shear deformations in the longitudinal layers are disregarded, while the contribution instead comes from the shear deformation of the cross layers.

The gamma method is complex to use for CLT with more than 5 layers. If the number of layers exceeds 5 layers and an extended version of the Gamma method is used [8].

Stiffness in the strong direction for a CLT plate with 5 layers

The gamma factors are calculated according to the following formulas. Here, the reduction factor, Ω, according to subsection 2.3 has been included in the conventional formulas to display how it is applied in calculations:

$$\gamma_1 = \frac{1}{\left(1 + \frac{\pi^2 E_1 t_1}{L_{ref}} \cdot \frac{t_2}{\Omega G_{r,2}}\right)} \tag{3.1}$$

$$\gamma_2 = 1 \tag{3.2}$$

$$\gamma_3 = \frac{1}{\left(1 + \frac{\pi^2 E_5 t_5}{L_{ref}^2} \cdot \frac{t_4}{\Omega G_{r,4}}\right)} \tag{3.3}$$

Distance from the midpoint of the i-layer to the center of gravity for the cross section:

$$a_1 = \left(\frac{t_1}{2} + t_2 + \frac{t_3}{2}\right) - a_3 \tag{3.4}$$

$$a_2 = \frac{\gamma_1 E_1 t_1 \left(\frac{t_1}{2} + t_2 + \frac{t_3}{2}\right) - \gamma_3 E_5 t_5 \left(\frac{t_3}{2} + t_4 + \frac{t_5}{2}\right)}{\gamma_1 E_1 t_1 + \gamma_2 E_3 t_3 + \gamma_3 E_5 t_5} \tag{3.5}$$

$$a_3 = \left(\frac{t_3}{2} + t_4 + \frac{t_5}{2}\right) + a_2 \tag{3.6}$$

The effective bending stiffness per width meter (m^4/m):

$$I_{x,\mathrm{ef}} = \frac{E_1}{E_{\mathrm{ref}}}\left(\frac{t_1^3}{12} + \gamma_1 t_1 a_1^2\right) + \frac{E_3}{E_{\mathrm{ref}}}\left(\frac{t_3^3}{12} + \gamma_2 t_3 a_2^2\right) + \frac{E_5}{E_{\mathrm{ref}}}\left(\frac{t_5^3}{12} + \gamma_3 t_5 a_3^2\right) \tag{3.7}$$

Stiffness in the weak direction for a CLT plate with 5 layers

The stiffness for a 5 layer CLT plate in the weak direction is calculated as a 3 layer CLT plate. The gamma factors can be calculated as formula (3.8) and (3.9). Where the reduction factor, Ω, is applied to the longitudinal modulus of elasticity for the y-direction, E_2 and E_4, according to subsection 2.3.

$$\gamma_1 = \frac{1}{1 + \frac{\pi^2 E_2 t_2}{L_{\mathrm{ref}}^2} \cdot \frac{t_3}{G_{r,3}}} \tag{3.8}$$

$$\gamma_2 = 1 \tag{3.9}$$

Distance from the midpoint of the i-layer to the center of gravity for the cross section:

$$a_1 = \left(\frac{t_2}{2} + t_3 + \frac{t_4}{2}\right) - a_2 \tag{3.10}$$

$$a_2 = \frac{\gamma_1 E_2 t_2 \left(\frac{t_2}{2} + t_3 + \frac{t_4}{2}\right)}{\gamma_1 E_2 t_2 + \gamma_2 E_4 t_4} \tag{3.11}$$

The effective bending stiffness per width meter (m^4/m):

$$I_{y,\mathrm{ef}} = \frac{E_2}{E_{\mathrm{ref}}}\left(\frac{t_2^3}{12} + \gamma_1 t_2 a_1^2\right) + \frac{E_4}{E_{\mathrm{ref}}}\left(\frac{t_4^3}{12} + \gamma_2 t_4 a_2^2\right) \tag{3.12}$$

3.1.2 Timoshenko theory

In the usage of Timoshenko beam theory for CLT design, the classic Bernoulli-Euler beam theory is used to calculate the bending stiffness, D_{EI}. In addition, an extension is introduced, regarding the shear stiffness, D_{GA}. Both of these stiffness parameters are taken into consideration when calculating the deflection. [9].

It is assumed that only the longitudinal layers contribute to the bending stiffness of the CLT, meaning that the cross layers do not provide any stiffness. However, for the shear stiffness, it is assumed that all the layers in the cross section are utilized [10].

Stiffness in the strong direction for a CLT plate with 5 layers

The bending stiffness per width meter ($\mathrm{Nm^2/m}$) is given by:

$$D_{EI_x} = E_{\text{ref}}\, I_{x,\text{net}} \tag{3.13}$$

Where $I_{x,\text{net}}$ is the net moment of inertia per width meter ($\mathrm{m^4/m}$) and is calculated as the following formula where i={1,3,5}:

$$I_{x,\text{net}} = \sum \left(\frac{t_i^3}{12} + t_i \cdot e_i^2 \right) \tag{3.14}$$

Here, e_i, is the distance between the midpoint of the specific layer to the center of gravity for the cross section.

The shear stiffness per width meter (N/m) can be calculated according to the following formula where n={1,3,5} and k={2,4}:

$$D_{GA_x} = \kappa_x \sum G_i t_i = \kappa_x \left(\sum G_{0,n} t_n + \sum \Omega G_{r,k} t_k \right) \tag{3.15}$$

Where κ is a shear correction factor and is calculated as [3]:

$$\kappa_x = \frac{\left(\sum (EI + EAa^2)\right)^2}{\sum G_i b t_i \cdot \int_h \frac{S^2(z)\, E^2(z)}{G(z)\, b(z)}\, dz} \tag{3.16}$$

Stiffness in the weak direction for a CLT plate with 5 layers

To calculate the bending stiffness, D_{EI_y} and the shear stiffness D_{GA_y} for the weak direction of a 5 layer CLT plate, the same formulas as for the strong direction can be applied and calculated as a 3 layer CLT plate.

3.1.3 Shear analogy method

In this method, the CLT plate is separated into two virtual beams, called beam A and beam B. Beam A represents the bending stiffness contribution due to the bending stiffness of the individual laminations. Beam B represents the bending stiffness contribution according to Steiner's theorem as well as the shear stiffness. Between these two beams, it is assumed to exist an infinite amount of rigid connectors, resulting in an equal deformation of the two beams.

The stiffnesses from beam A and beam B are then added and gives the effective bending stiffness, $(EI)_{ef}$. Which in turn can be used for calculations in the ultimate limit state and serviceability limit state along with an effective shear stiffness, $(GA)_{ef}$ [11].

Stiffness in the strong direction for a CLT plate with 5 layers

The effective bending stiffness in the strong direction per width meter (Nm^2/m) can be determined using the following formula:

$$(EI)_{ef,x} = B_A + B_B \tag{3.17}$$

Where B_A and B_B are calculated as the following formulas where i={1,3,5}:

$$B_A = \sum E_i \frac{t_i^3}{12} \tag{3.18}$$

and:

$$B_B = \sum E_i \, t_i \, z_i^2 \tag{3.19}$$

respectively. Here, z_i, is the distance between the midpoint of the specific layer to the center of gravity for the cross section.

The effective shear stiffness per width meter (N/m) can be determined using the following formula, where $n = 5$ and $i = \{2, 3, 4\}$, with the reduction factor, Ω, being applied for $i = 2$ and $i = 4$ [11]:

$$(GA)_{ef,x} = \frac{\left(h - \frac{t_1}{2} - \frac{t_n}{2}\right)^2}{\left(\frac{t_1}{2 \cdot G_1} + \sum \frac{t_i}{G_i} + \frac{t_n}{2 \cdot G_n}\right)} \tag{3.20}$$

Stiffness in the weak direction for a CLT plate with 5 layers

To calculate the bending stiffness, $(EI)_{ef,y}$ and the shear stiffness $(GA)_{ef_y}$ for the weak direction of a 5 layer CLT plate, the same formulas as for the strong direction can be applied and calculated as a 3 layer CLT plate.

3.2 2D – Plate

3.2.1 Mindlin-Reissner plate theory

One way to model a CLT plate in 2D is to use orthotropic Mindlin-Reissner plate theory. This is due to the structural composition of the CLT, making the behavior ideally represented as an orthotropic material. Mindlin-Reissner plate theory can be considered the 2D version of Timoshenko beam theory, being designated as a shear flexible thick plate. [9]. The stiffness for a 2D CLT plate can be expressed by the relation between the internal forces and their conjugate generalized strains according to the following matrix. The internal forces are expressed as force respectively moment per width meter [3].

$$\begin{bmatrix} m_x \\ m_y \\ m_{xy} \\ v_{xz} \\ v_{yz} \\ n_x \\ n_y \\ n_{xy} \end{bmatrix} = \begin{bmatrix} D_{11} & D_{12} & 0 & 0 & 0 & 0 & 0 & 0 \\ D_{21} & D_{22} & 0 & 0 & 0 & 0 & 0 & 0 \\ 0 & 0 & D_{33} & 0 & 0 & 0 & 0 & 0 \\ 0 & 0 & 0 & D_{44} & 0 & 0 & 0 & 0 \\ 0 & 0 & 0 & 0 & D_{55} & 0 & 0 & 0 \\ 0 & 0 & 0 & 0 & 0 & D_{66} & D_{67} & 0 \\ 0 & 0 & 0 & 0 & 0 & D_{76} & D_{77} & 0 \\ 0 & 0 & 0 & 0 & 0 & 0 & 0 & D_{88} \end{bmatrix} \begin{bmatrix} K_x \\ K_y \\ K_{xy} \\ \gamma_{xz} \\ \gamma_{yz} \\ \varepsilon_x \\ \varepsilon_y \\ \gamma_{xy} \end{bmatrix} \tag{3.21}$$

where the stiffness parameters are related to following type of load application:
$D_{11} - D_{33}$: bending and torsional stiffness, kNm/m
$D_{44} - D_{55}$: out of plane shear stiffness, kN/m
$D_{66} - D_{88}$: axial stiffness and in plane shear stiffness, kN/m

Furthermore, it is assumed that the following stiffness parameters are set to 0 in the matrix as the transverse expansion for CLT is generally neglected [9].

$$D_{12} = D_{21} = D_{67} = D_{76} = 0$$

The internal forces acting on the plate, i.e. the left hand side of equation (3.21) are visualized in figure 3.1. Note that the figure expresses the out of plane shear as n_{xz} and n_{yz}, however, in this project they will be expressed as v_{xz} and v_{yz} respectively.

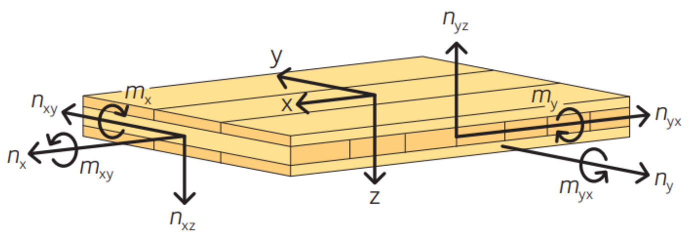

Figure 3.1: Visualization of loads acting on the plate [3]

Furthermore, the displacement measures, can also be expressed as the following:

$$\begin{bmatrix} K_x \\ K_y \\ K_{xy} \\ \gamma_{xz} \\ \gamma_{yz} \\ \varepsilon_x \\ \varepsilon_y \\ \gamma_{xy} \end{bmatrix} = \begin{bmatrix} \frac{\partial \phi_y}{\partial x} \\ -\frac{\partial \phi_x}{\partial y} \\ \frac{\partial \phi_y}{\partial y} - \frac{\partial \phi_x}{\partial x} \\ \frac{\partial u_z}{\partial x} + \phi_y \\ \frac{\partial u_z}{\partial y} - \phi_x \\ \frac{\partial u_x}{\partial x} \\ \frac{\partial u_y}{\partial y} \\ \frac{\partial u_x}{\partial y} + \frac{\partial u_y}{\partial x} \end{bmatrix} \tag{3.22}$$

Where u and ϕ in equation in (3.22) represents translations and rotations respectively [3]. Furthermore, the ∂ symbol represents the partial derivative with respect to the spatial coordinates. To display how to interpret the formulas and how they could be applied in this project, two examples are showcased.

- **Strain in the x-direction, ε_x:** An elongation in the x-direction of a plate with initial length $L_0 = 1$ m can be achieved by applying a unit translation $u_x = 1$. This is done by e.g. applying $u_x = 0.5$ mm at one end and $u_x = -0.5$ mm at the other end. The axial strain is then calculated as:

$$\varepsilon_x = \frac{\partial u_x}{\partial x} = \frac{L_{new} - L_0}{L_0} = \frac{0.001}{1} = 0.001 \tag{3.23}$$

- **Curvature due to bending around the y-direction, K_x:** A curvature K_x of a plate with initial length $L_0 = 1$ m is achieved by applying a unit rotation $\phi_y = 1$ rad. This is done by e.g. applying $\phi_y = 0.5$ rad at one end and $\phi_y = -0.5$ rad at the other end. The curvature is then calculated as:

$$K_x = \frac{\partial \phi_y}{\partial x} = \frac{\Delta \phi_y}{L_0} = \frac{1}{1} = 1 \tag{3.24}$$

3.3 3D – Finite element analysis

Regarding 3D modeling of CLT, there are multiple finite element analysis programs, and the most suitable option varies depending on the purpose of the practical usage. For example, programs such as RFEM or FEM-design have a purpose in design, while Abaqus has a purpose in teaching and research [3].

The way in which the modeling is done also varies, depending on the program in question. How the models for this project were created in Abaqus [12] and in FEM-design [13] will be explained in detail in the respective subchapters below.

3.3.1 Shell model creation in FEM-design

To create the model in FEM-design, shown in figure 3.2, the following steps are performed:

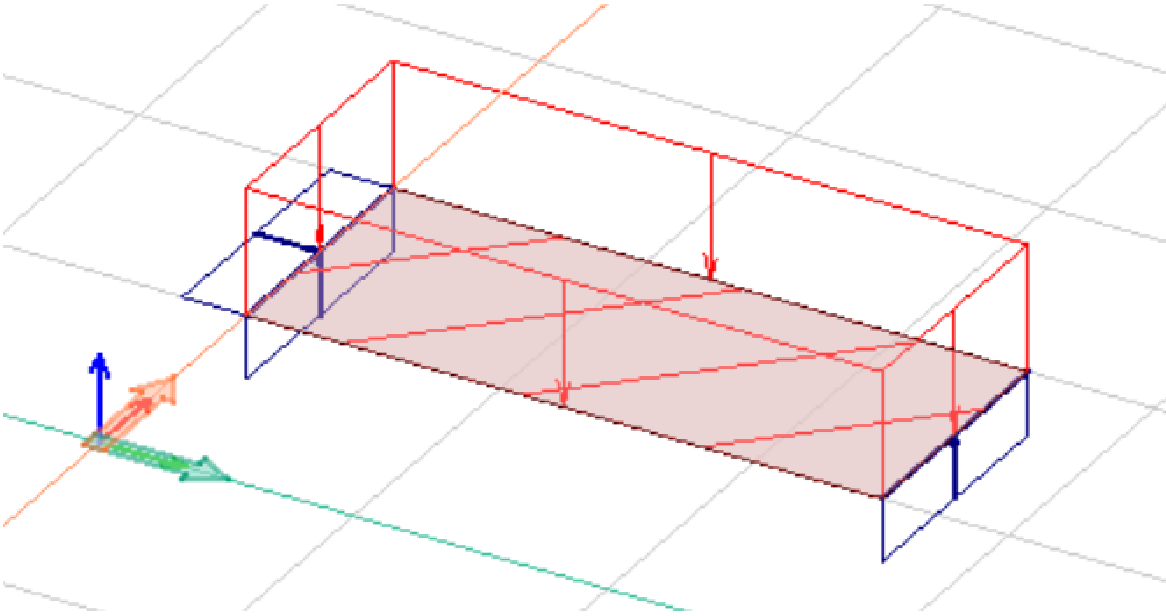

Figure 3.2: Visualization of the model in FEM-design

Step 1 - Structure

As two different methods are used when creating the structure, this step differs as the command "fictitious shell" is chosen in the structure toolbar. Here, the possibility of defining a stiffness matrix of an orthotropic material is available, where the user can determine a stiffness matrix for the structure, more on this in section 3.4.

The second method is the possibility of choosing the timber shell module, where predetermined CLT configurations can be used. Here, the predetermined configurations can be modified, i.e. modify the layer thicknesses and stiffness's to a desired value, see figure 3.3. Consequently, the material stiffness of a specific layer can also be reduced to represent the gaps according to section 2.3, similarly to how the gaps are taken into consideration for the analytical methods. The program itself then creates and utilizes a stiffness matrix dependent on the values in figure 3.3

No.	Material	Thickness [mm]	Θ [°]	Ex [N/mm²]	Ey [N/mm²]	v xy [-]	Gxy [N/mm²]	Gxz [N/mm²]	Gyz [N/mm²]	ρ [kg/m³]
1	C24	40.00	0.00	11000	0.00	0.00	690	690	50	420
2	C24	40.00	90	11000	0.00	0.00	690	690	50	420
3	C24	40.00	0.00	11000	0.00	0.00	690	690	50	420
4	C24	40.00	90	11000	0.00	0.00	690	690	50	420
5	C24	40.00	0.00	11000	0.00	0.00	690	690	50	420

Figure 3.3: Parameter modifier for the method FEM-design, timber module

Step 2 - Loads

In the load toolbar, an uniform surface load and line supports are applied according to the conditions of the design case found in section 5.1. The line supports represents a simply supported plate, as seen in figure 3.2 The applied load is then included in a load case where the load type and duration class are specified. Henceforth, the load class is included in a load combination where the type of load combination is specified.

Step 3 - Finite elements

In this step, a finite element mesh is generated, which can be done automatically by the command "prepare". The mesh can then be altered to be finer if needed.

Step 4 - Analysis

Lastly, the created load case or load combination is chosen to be included in the calculation command. For the fictitious shell, the internal forces and displacements are then observed in the results menu which is part of the quick tools bar. For the timber shell, the design stresses can also be extracted directly. The extracted values are then used for evaluation according to section 4.1 and 4.2.

3.3.2 3D Model creation in Abaqus

The 3D model of the CLT plate is done in Abaqus, a visualization of how the finished model can look like, is illustrated in figure 3.4.

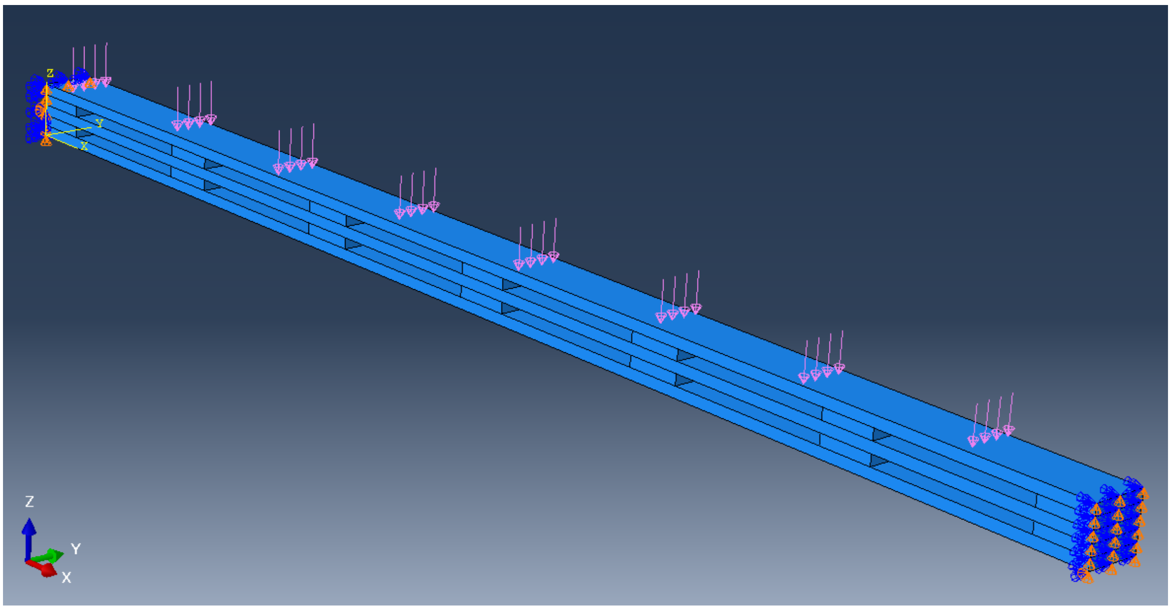

Figure 3.4: Visualization of full 3D model, reduced due to symmetry

Notably, the entire width of the CLT plate has not been included in the model, as a symmetry cut can be utilized to enable a finer mesh. The 3D model can be created by doing the following steps:

Step 1: Part module

Multiple parts are created, representing each layer with their specific thickness. As the CLT in question is non edge glued, lamellas need to be created in the model. This is done by the introduction of datum planes, which are used as partion tools to define the individual lamellas. This is only done for the cross layers as the symmetry cut is made so that the width of exactly one lamella is modeled for the longitudinal layer.

Step 2: Property module

In the property module, a material is created, where the mechanical properties are chosen to be defined as an elastic material by engineering constants. The values for the stiffness parameters are found in table 2.2 and have the following corresponding notations in the software, defined according to the orientations in figure 2.1:

- $E_0 = E_L$
- $E_{90} = E_R = E_T$
- $G_0 = G_{LR} = G_{LT}$
- $G_R = G_{RT}$

Other than creating a material, a homogeneous section is created and assigned to the model. The orientations also need to be assigned according to subsection 2.1.1.

Step 3: Step module

A step is created, chosen to be static, linear perturbation. However, when checking the frequency, the frequency step is chosen.

Step 4: Assembly module

As the parts are assembled, the lamellas are connected through the command "Cut and merge" which merges together all the separate parts. This is to avoid using tie constraints between the layers in the interaction module. The main benefits are that it is faster to model, and possible complications between the main and secondary surfaces are avoided.

Step 5: Load module

In the load module, a surface load according to section 5.1 is applied, along with the boundary conditions which are deemed to realistically represent a simply supported beam, as used for the analytical methods. Since the 3D model in Abaqus allows local indentation, the deflection would be overestimated compared to the other methods. To avoid this, boundary conditions are applied with the purpose of restraining the deflection in the z-direction along the height of the plate.

This is done by restraining the displacement in the z-direction (U3=0) at the end surfaces of the three longitudinal layers, as shown in figure 3.4. Along with this, for the model to be simply supported, the displacement in the x-direction is also restrained (U1=0), on a line in the middle of the cross section at one of the end surfaces. [14].

In addition to this, boundary conditions which prevent rigid body motions are added and restrained in the y-direction (U2=0). These boundary conditions are added on both end edges of the plate, on the surface of the most central lamella.

Step 6: Mesh module

The mesh element type is chosen to be an eight node brick element (C3D8). It is important to use a mesh that is both fine and time efficient, therefore, a mesh size of a specific model is chosen according to a convergence study in subsection 5.3.

Step 7: Job module

A job is created and submitted.

Step 8: Visualization module

In the visualization module for the 3D model, the resulting design stresses, frequency and deflections are observed. These values will later be applied according to section 4.1 and section 4.2 respectively.

When observing the design stresses, stress concentrations for nodes at the edge of the gaps tend to increase linearly with the number of mesh elements. Therefore, the stress value for adjacent nodes are chosen instead.

The values from the stress components S11, S13 and S23 is collected as they represent the design stresses examined for the design case in subsection 4.1. They represent the design bending stress, design longitudinal shear stress and design rolling shear stress respectively.

3.4 Homogenization

3.4.1 The method of homogenization

Homogenization is an important part of the project, as it is an essential step to achieve the stiffness matrix for use in FEM-design. The process of homogenization means to transform a heterogeneous material, like CLT, to a homogeneous material [15]. By definition, usage of the Gamma method, Timoshenko theory and Shear analogy method is a homogenization because a representative bending and, shear stiffnesses are assigned the entire plate. Furthermore, the homogenized stiffnesses for the material can then be expressed and defined as part of a stiffness matrix. Multiple methods exist for the usage of homogenization, in addition to the previously mentioned methods, it can also be done with the help of 3D finite element analysis [16]. For this project, the FE-software Abaqus is used.

In this project, homogenization is needed in order to perform and achieve both main purposes. As a result of the homogenization, the stiffness matrix of the "Gap CLT" can be determined, which in turn is plugged into FEM-design. Therefore, homogenization can contribute to a comparison between the different design methods, by providing the possibility of using FEM-design for this purpose. Furthermore, it also provides the opportunity to do a deep dive in FEM-design, exploring the possibilities and limitations of the "Gap CLT".

The homogenization is partly performed by modeling the "Gap CLT" in the FE-software Abaqus, using the representative volume element (RVE). This method involves creating a small representative volume instead of modeling the entire 3D CLT plate, as shown in figure 3.6. The stiffness parameter can be determined according to 2D orthotropic Mindlin-Reissner plate theory, using matrix (3.21).

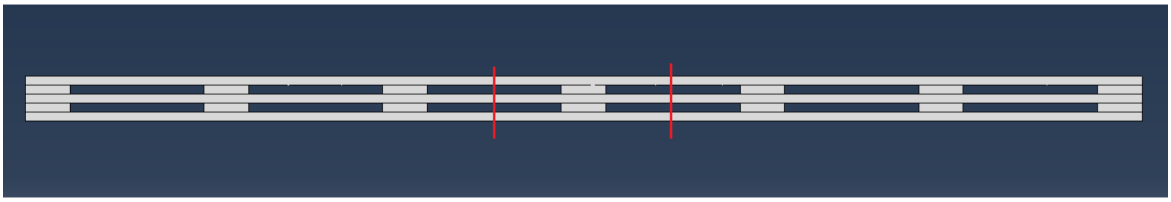

Figure 3.5: Illustration of a RVE-model being a representative volume element of the entire CLT plate due to symmetry.

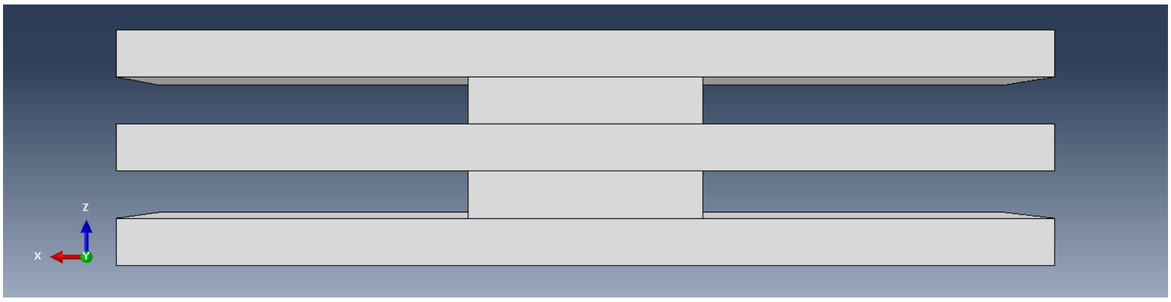

Figure 3.6: Example of RVE-model for "gap CLT"

To further expand on the RVE-model shown in figure 3.6, the principle of the model being a representative volume, means that exact copies of the RVE-model could be placed directly next to each other in the xy-plane in an infinite number, without altering the deformation pattern at loading.

The ends of the model represent symmetry planes, meaning that the gaps are exactly twice the length in the longitudinal direction, compared to what is shown in figure 3.6.

For a CLT plate without gaps (or very small gaps) the resulting RVE-model would be almost perfectly cube-shaped. With the exception of slightly longer longitudinal layers, to avoid trouble between the constraints surfaces mentioned in subsection 3.4.2 and seen in figure 3.7.

To determine all the stiffness parameters in the matrix, two things are needed according to matrix (3.21), the internal forces and the displacements. Using the RVE-models, a set of unit displacement are used to observe the corresponding reaction forces. For each case of unit displacement, the reaction forces represent one column of the stiffness matrix (3.21). As an example, for the case $\varepsilon_x = 1$, all the other displacement measures such as ε_y, γ_{xz} and K_x are equal to 0. When all the relevant stiffness parameters are known, the stiffness matrix will be complete and ready to be plugged into FEM-design for usage.

To expand on the showcase of the determination of the displacement by equation (3.23) in subsection 3.2. A stiffness parameter in matrix (3.21) can be calculated according to the following principle. Where RF is the observed reaction force, ϵ_x is the strain in the x-direction and B is the width of the RVE-model.

$$\frac{RF}{B} = D \cdot \varepsilon_x \tag{3.25}$$

With insertion of equation (3.23) into equation (3.25), it can be rearranged and expressed according to equation (3.26). L_{new} and L_0 are the deformed and initial lengths of the RVE-model, respectively:

$$D = \frac{RF}{B \cdot \frac{L_{new} - L_0}{L_0}} \tag{3.26}$$

3.4.2 RVE-model creation in Abaqus

This model creation for RVE-models is very similar to the creation of the 3D model also created in Abaqus. Therefore, for a complete explanation of how to create the model, see subsection 3.3.2. However, the following modules are either done differently or added for the creation and usage of the RVE model:

- **Part module:** There is no need for datum planes or partition tools while creating the RVE model.
- **Interaction module:** Reference points (RP) are applied in the middle of each side of the RVE-model. Then distributed coupling constraints are applied, where the reference points are chosen to be the main surface and the layer surfaces are chosen to be the secondary surfaces, see figure 3.7. Note that the constraints are applied for the three end surfaces in the yz-plane when representing the symmetry cut of the lamellas in the x-direction. For the symmetry cut of the lamellas going in the ¡y-direction, only the two surfaces for layer 2 and layer 4 are constrained. The constraints that most realistically represent a CLT plate as a RVE-model are showcased in the results part.
- **Load module:** The boundary conditions and the unit displacements are applied in the reference points, which in turn are then controlled by the constraints. The boundary conditions that most realistically represent a CLT plate as a RVE-model are showcased in subsection 3.4.3.
- **Visualization module:** In the visualization module, the reaction forces and reaction moments are to be observed. This is done at the reference points through the field output.
- **Create the stiffness matrix:** As the reaction forces and reaction moments have been observed, calculations to determine the stiffness parameter are made. An example of how they are calculated is showcased in equation (3.26) in subsection 3.4.1. These stiffness calculations along with displacements calculations are done in Excel, where a stiffness matrix is set up to easily extract values to the fictitious shell in FEM-design. The determined stiffness matrices are compiled in the result part.

3.4.3 Boundary conditions and constraints

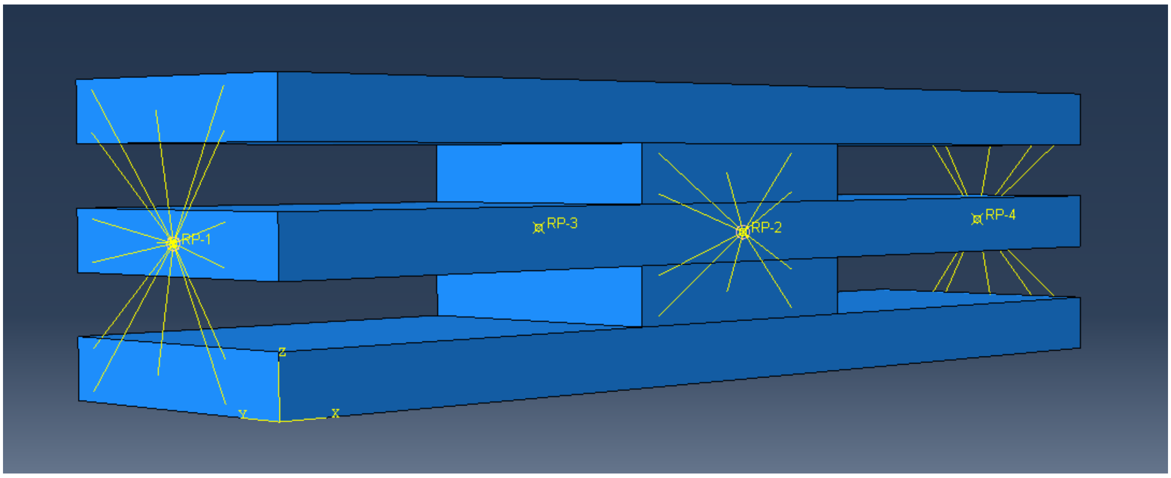

Figure 3.7: Showcase of constraints and its reference points where boundary conditions are attached

Figure 3.7 is used as a reference to understand which boundary conditions, constraints and displacement are applied at a specific reference points for respective case. In the following section, the applied unit displacements and the restrained boundary conditions are showcased and compiled. Table 3.1 and table 3.2 showcase the constrained translations and rotation at the reference points shown in figure 3.7, for each case of unit displacement. While in table 3.3 to table 3.10, the boundary conditions for each case of unit displacement are displayed.

Table 3.1: Applied distributed constraints for RP1 and RP4 in the RVE-models

	U1	U2	U3	UR1	UR2	UR3
m_x	0	0	0	0	0	0
m_y	-	-	-	-	-	-
m_{xy}	0	0	0	0	-	-
v_{xz}	0	0	0	0	0	0
v_{yz}	-	-	-	-	-	-
n_x	0	0	0	0	0	0
n_y	-	-	-	-	-	-
n_{xy}	0	0	0	-	-	-

Table 3.2: Applied distributed constraints for RP2 and RP3 in the RVE-models

	U1	U2	U3	UR1	UR2	UR3
m_x	-	-	-	-	-	-
m_y	0	0	0	0	0	0
m_{xy}	0	0	0	-	0	-
v_{xz}	-	-	-	-	-	-
v_{yz}	0	0	0	0	0	0
n_x	-	-	-	-	-	-
n_y	0	0	0	0	0	0
n_{xy}	0	0	0	-	-	-

The RVE-models representing torsion, m_{xy} and in plane shear, n_{xy}, unit displacement is applied at all sides of the RVE-model as it has shown to give the most realistic results. The unit displacement at the cross layers needs to be divided by the relation:

$$\varsigma = L_{RVE}/B_{RVE}.$$

Where L_{RVE} is the length of the RVE-model, in the x-direction and B_{RVE} is the width of the RVE model, in the y-direction.

The following three tables represent the unit displacement case for the flexural stiffness:

Table 3.3: Applied boundary conditions for bending in the x-direction in the RVE-model

Bending in x-direction, m_x	U1	U2	U3	UR1	UR2	UR3
Reference point 1	0	0	0	0	-0.5	0
Reference point 2	-	-	-	-	-	-
Reference point 3	-	-	-	-	-	-
Reference point 4	0	0	0	0	0.5	0

Table 3.4: Applied boundary conditions for bending in the y-direction in the RVE-model

Bending in y-direction, m_y	U1	U2	U3	UR1	UR2	UR3
Reference point 1	-	-	-	-	-	-
Reference point 2	0	0	0	0.5	0	0
Reference point 3	0	0	0	-0.5	0	0
Reference point 4	-	-	-	-	-	-

Table 3.5: Applied boundary conditions for twist around the x-axis in the RVE-model

Twist around the x-axis, m_{xy}	U1	U2	U3	UR1	UR2	UR3
Reference point 1	0	0	0	-0.5	0	0
Reference point 2	0	0	0	0	$0.5/\varsigma$	0
Reference point 3	0	0	0	0	$-0.5/\varsigma$	0
Reference point 4	0	0	0	0.5	0	0

The following 2 tables represent the unit displacement case for the out of plane shear stiffness:

Table 3.6: Applied boundary conditions for out of plane shear in the RVE-model

Out of plane shear, v_{xz}	U1	U2	U3	UR1	UR2	UR3
Reference point 1	0	0	0.5	0	0	0
Reference point 2	-	-	-	-	-	-
Reference point 3	-	-	-	-	-	-
Reference point 4	0	0	-0.5	0	0	0

Table 3.7: Applied boundary conditions for out of plane shear in the RVE-model

Out of plane shear, v_{yz}	U1	U2	U3	UR1	UR2	UR3
Reference point 1	-	-	-	-	-	-
Reference point 2	0	0	0.5	0	0	0
Reference point 3	0	0	-0.5	0	0	0
Reference point 4	-	-	-	-	-	-

The following 2 tables represent the unit displacement case for the membrane stiffness:

Table 3.8: Applied boundary conditions for elongation in the x-direction in the RVE-model

Elongation in x-direction, n_x	U1	U2	U3	UR1	UR2	UR3
Reference point 1	-0.5	0	0	0	0	0
Reference point 2	-	-	-	-	-	-
Reference point 3	-	-	-	-	-	-
Reference point 4	0.5	0	0	0	0	0

Table 3.9: Applied boundary conditions for elongation in the y-direction in the RVE-model

Elongation in y-direction, n_y	U1	U2	U3	UR1	UR2	UR3
Reference point 1	-	-	-	-	-	-
Reference point 2	0	-0.5	0	0	0	0
Reference point 3	0	0.5	0	0	0	0
Reference point 4	-	-	-	-	-	-

Lastly, the last table represent unit displacement case of in plane shear stiffness.

Table 3.10: Applied boundary conditions for in plane shear in the RVE-model

In plane shear, n_{xy}	U1	U2	U3	UR1	UR2	UR3
Reference point 1	0	0.5	0	0	0	0
Reference point 2	$0.5/\varsigma$	0	0	0	0	0
Reference point 3	$-0.5/\varsigma$	0	0	0	0	0
Reference point 4	0	-0.5	0	0	0	0

4 CLT Design

In the ultimate limit state, structures are checked if they have sufficient capacity to withstand structural failure. While in the serviceability limit state, it must be proven that the structure has a sufficient functional performance level. All formulas seen in the following subsection are in regards to a simply supported CLT plate with 5 layers.

4.1 Ultimate limit state

4.1.1 Bending moment check

The maximum bending moment acting on the plate is calculated according to the following formula, with the surface load, q_d :

$$m_{x,d} = \frac{q_d L^2}{8} \tag{4.1}$$

The design bending stresses are calculated according to the following formula.

$$\sigma_{m_x,d} = \frac{m_{x,d}}{W_{x,\text{net}}} \tag{4.2}$$

Where the bending resistance, $W_{x,\text{net}}$, is determined as shown below. Furthermore, the net moment of inertia is determined as shown in subsection 3.1.2 and z_{max} is the maximum distance from the center of the cross section to the outer edge of the cross section, symmetry is assumed:

$$W_{x,\text{net}} = \frac{I_{x,\text{net}}}{z_{\text{max}}} \tag{4.3}$$

However, for calculations according to the Gamma method, the design bending stresses can be calculated according to formula (4.4):

$$\sigma_{m_x,d} = \left(\gamma_3 \alpha_3 + \frac{t_5}{2}\right) \cdot \frac{m_{x,d}}{I_{x,\text{ef}}} \tag{4.4}$$

The design criterion reads:

$$\sigma_{m_x,d} < f_d \tag{4.5}$$

with the design strength, f_d, according to section 2.2.2 [11].

4.1.2 Longitudinal shear check

The maximum shear force is calculated as:

$$v_{xz,d} = \frac{q_d \cdot L}{2} \tag{4.6}$$

Which gives the design longitudinal shear stresses:

$$\tau_{xz,d} = \frac{S_x\, v_{x,z,d}}{I_{x,net}} \tag{4.7}$$

Where the static moment, S_x, is calculated as shown below. The distance $e_{x,1}$ is calculated as stated in subsection 3.1.2:

$$S_x = t_1\, e_1 + \frac{t_3^2}{8} \tag{4.8}$$

However, for calculations according to the Gamma method, the design longitudinal shear stresses can be calculated according to formula 4.9.

$$\tau_{xz,d} = \left(\gamma_3 a_3 t_5 + \frac{t_3^2}{8}\right) \frac{v_{x,z}}{I_{x,\mathrm{ef}}} \tag{4.9}$$

The design criterion reads:

$$\tau_{xz,d} < f_d \tag{4.10}$$

with the design strength, f_d, according to subsection 2.2.2 [17].

4.1.3 Rolling shear check

With the maximum shear force according to equation (4.6), the design rolling shear stresses are calculated as the following:

$$\tau_{xz,r,d} = \frac{S_{xr}\, v_{xz,d}}{I_{x,\mathrm{net}}} \tag{4.11}$$

Where the static moment, $S_{x,r}$, is calculated as following:

$$S_{x,r} = t_1\, e_1 \tag{4.12}$$

However, for calculations according to the Gamma method, the design bending stresses can be calculated according to formula (4.13).

$$\tau_{xz,r,d} = \gamma_1 a_1 t_1 \frac{v_{xz,d}}{I_{x,\mathrm{ef}}} \tag{4.13}$$

The design criterion reads:

$$\tau_{xz,r,d} < f_d \tag{4.14}$$

with the design strength, f_d, according to subsection 2.2.2 [17].

4.2 Serviceability limit state

4.2.1 Deflection

For the deflection, the contribution from both characteristic loading (permanent damage) and quasi-permanent loading (long term damage) needs to be accounted for. The final deflection, w_{fin}, can then be determined as the following:

$$w_{\text{fin}} = w_{\text{inst}} + w_{\text{creep}} \tag{4.15}$$

Furthermore, the load reduction factors, ψ, needed for this section, are chosen according to subsection 2.2.1.

Instantaneous deflection

As for the instantaneous deflection, it is determined differently depending on the design theory used. The contribution from both permanent loads and live loads needs to be added according to the following formula:

$$w_{\text{inst}} = w_{inst,g} + \psi_0 \cdot w_{inst,q} \tag{4.16}$$

For the gamma method, deformation is determined as:

$$w_{\text{inst,g}} = \frac{5\, g_k\, L^4}{384\, D_{EI,ef}} \tag{4.17}$$

and:

$$w_{\text{inst,q}} = \frac{5\, q_k\, L^4}{384\, D_{EI,ef}} \tag{4.18}$$

For the Timoshenko theory and shear analogy method, deformation is calculated as:

$$w_{\text{inst,g}} = \frac{5\, g_k\, L^4}{384\, D_{EI}} + \frac{g_k\, L^2}{8\, D_{GA}} \tag{4.19}$$

and:

$$w_{\text{inst,q}} = \frac{5\, q_k\, L^4}{384\, D_{EI}} + \frac{q_k\, L^2}{8\, D_{GA}} \tag{4.20}$$

Long term deflection

Where the deflection in regard to long term effects, w_{creep}, is determined according to equation (4.21). Furthermore, the value of k_{def} is determined according to subsection 2.2.1:

$$w_{\text{creep}} = k_{\text{def}}(w_{\text{inst}} + \psi\, w_{\text{inst}}) \tag{4.21}$$

Limits

The limit for the instantaneous deflection can be determined according to equation (4.22), where the length is divided by 400, according to recommendations:

$$w_{inst,lim} = \frac{L}{400} \tag{4.22}$$

The limit for the final deflection is chosen as the length divided by 300, according to recommendations [3]:

$$w_{fin,lim} = \frac{L}{300} \tag{4.23}$$

4.2.2 Frequency

The frequency of the CLT plate should also be checked. If the first frequency is above 8 Hz, then the checks in regards to velocity and unit load criterion need to be checked. However, if the first frequency is below 8 Hz, the same checks need to be done, along with an additional check in regards of acceleration. Furthermore, the lower limit for the frequency that must be fulfilled is 4.5 Hz [17].

$$f_1 = \frac{\pi}{2L^2}\sqrt{\frac{D_{\mathrm{EI},x}}{m}} \tag{4.24}$$

Where m is the mass per square meter, however, it is not sufficient to simply include the self weight of the plate. External mass in the form of loads acting on the plate must also be taken into account [9]. The included contribution to m by the loads acting on the plate are 100 % of the permanent load along with 20 % of the live load.

4.2.3 Velocity

The modal impulse from a footstep on the plate can be determined by equation (4.25), where the step frequency, f_w, is assumed to be 2 Hz:

$$I_{mod,mean} = \frac{42 f_w^{1.43}}{f_1^{1.3}} \tag{4.25}$$

Furthermore, the maximum velocity, caused by the impulse, is calculated according to formula (4.26), where B is the width:

$$v_{1,peak} = k_r \frac{I_{mod,mean}}{\frac{mBL}{2} + 70} \tag{4.26}$$

Where $k_{red} = 0.7$ and is determined according to subsection 4.2.2.

While the total maximum velocity is calculated as shown below:

$$v_{tot,peak} = k_{imp} v_{1,peak} \tag{4.27}$$

Where the factor k_{imp} is determined as:

$$k_{imp} = max\left(0.48(\frac{B}{L})\left(\frac{D_{EI,x}}{D_{EI,y}}\right)^{0.25}, 1\right) \tag{4.28}$$

The final velocity response, v_{rms}, is then determined by:

$$v_{rms} = v_{tot,peak}(0.65 - 0.01f_1)(1.22 - 11\zeta)\eta \tag{4.29}$$

Where ζ is a factor dependent on the modal damping of the plate, and η is a factor that is determined according to the following:

$$\eta = 1.34 - 0.4k_{imp} \tag{4.30}$$

The performance level of the plate depends on the limit $v_{rms,lim}$ displayed in table 4.1 [17].

Table 4.1: Performance level, velocity, in m/s

Performance								
Level	I	II	III	IV	V	VI	VII	VIII
$v_{rms,lim}$	0.0004	0.0008	0.0012	0.0016	0.0024	0.0036	0.0042	0.0048

4.2.4 Unit load criterion

The unit load criterion is based on checking the deflection due to a 1 kN vertical load at the most disadvantageous point and is calculated according to formula (4.31):

$$w_{1kN} = \frac{F \cdot L^3}{48 \cdot D_{EI,x} \cdot B_{ef}} \tag{4.31}$$

Where the effective width is calculated by the following formula:

$$B_{ef} = min\left(0.95L\left(\frac{D_{EI,y}}{D_{EI,x}}\right)^{0.25}, B\right) \tag{4.32}$$

Finally, the maximum allowed deflection w_{lim} and the corresponding performance level is given as shown in table 4.2 [17].

Table 4.2: Performance level, point load criterion, deflection in mm

Performance								
Level	I	II	III	IV	V	VI	VII	VIII
$w_{1kN,lim}$	0.25	0.25	0.5	1	1.25	1.5	1.75	2

5 Results

5.1 Preconditions of design case

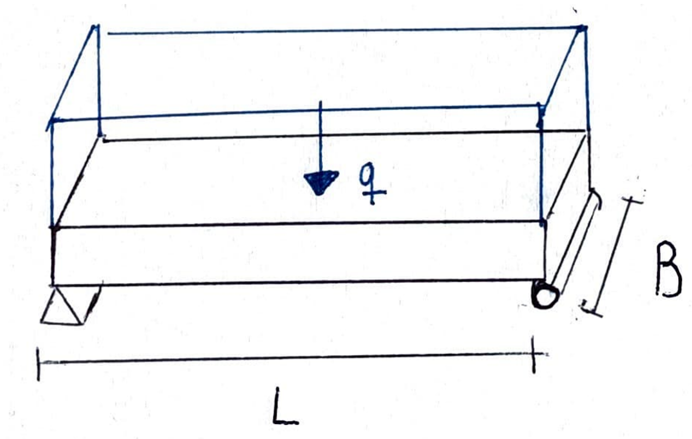

Figure 5.1: Illustration of the design case

A design case is chosen to be studied for calculations in the ultimate limit state and serviceability limit state. The conditions for the design case are compiled below.

- Length of the plate: $L = 5$ m
- Width of the plate: $B = 2$ m
- Width of lamellas: 0,2 m
- Permanent load acting on the plate: $g_{k,1} = 1.5\frac{kN}{m^2}$
- Self weight of the plate as: $g_{k,2} = g\rho V$
- Live load acting on the plate: $q_k = 2.0\frac{kN}{m^2}$

Where the density $\rho = 420$ kg/m^3 and the design load is calculated according to STR.B [4] and the safety class factor according to section 2.2.1:

$$q_d = \gamma_d \cdot (1.2 \cdot (g_{k,1} + g_{k,2}) + 1.5 \cdot q_k) \tag{5.1}$$

The case study will be performed by comparing calculations for six different modeling methods. As mentioned previously, the calculations will be done in the ultimate limit state and the serviceability limit state for each of the six methods. In this chapter, the results will be compiled and presented. For how the modeling was done according to the different methods, see chapter 3. While the formulas used for calculation in the ultimate limit state and the service limit state, see chapter 4. The six methods that will be presented and compared are calculations according to modeling with:

- Gamma method
- Timoshenko theory
- Shear analogy method
- FEM-design 1, fictitious shell
- FEM-design 2, timber module
- Abaqus

The first three will be performed in Excel and the other three are finite element analysis and will henceforth be performed in the respective program. Although Abaqus will also be used to determine the stiffness matrix, which will be needed for the fictitious shell in FEM-design, as explained in section 3.4 respectively in subsection 3.3.1.

5.2 Configurations

The four CLT configurations that are being investigated are results achieved by optimization in ultimate limit state and serviceability limit state through the analytical methods in Excel and preconditions mentioned in subsection 5.1. The reason for using four different configurations was to have a basic standard CLT plate, configuration 1, to be used as a reference in comparison to an optimized product. It was then decided to optimize the CLT plate with three separate principles, to better understand the effect of introducing gaps compared to changing layer thicknesses and possibilities in terms of material saving. The three principles are:

- Conifguration 2: Optimization through gaps only.
- Conifguration 3: Optimization through changing layer thicknesses only.
- Conifguration 4: Optimization through gaps and changing layer thicknesses.

The optimization was done by trial and error for each configuration by changing the reduction factor due to size of the gaps, respectively, the layer thicknesses, which was changed with an increment of 5 mm. I.e. if another lamella was removed in configuration 2, it would fail the design check due to the further reduced reduction factor. For the design check to be considered to fail, only one of the checks mentioned in chapter 4 would need to exceed its limit.

For this specific design case with preconditions according to 5.1, the minimum frequency limit of 8 Hz was shown to be the first limit to be exceeded. This meant that frequency became the governing design check and the creation of the geometry for the different configuration was optimized with the intent of keeping the frequency above the 8 Hz limit.

The resulting configurations for the design case are visualized in subsection 5.2.1 along with detailed geometric information subsection 5.2.2.

5.2.1 Visualization

Configuration 1: Standard 40 mm x 5 layer CLT plate.

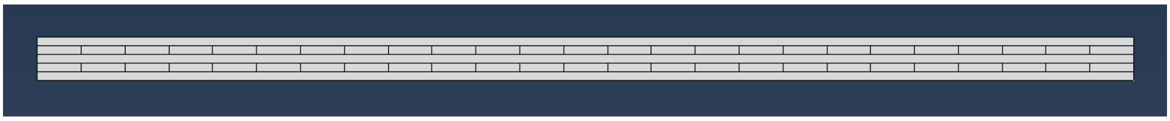

Figure 5.2: Visualization of configuration 1 in Abaqus

Configuration 2: CLT plate optimized with gaps only.

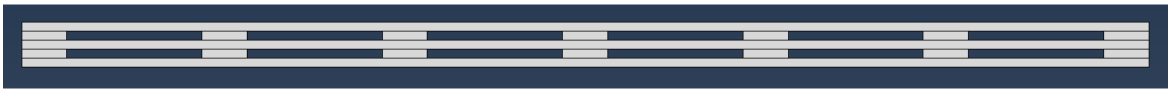

Figure 5.3: Visualization of configuration 2 in Abaqus

Configuration 3: CLT plate optimized by changing layer thickness only.

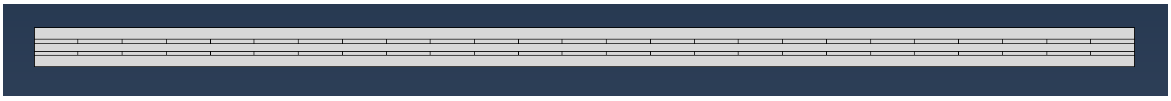

Figure 5.4: Visualization of configuration 3 in Abaqus

Configuration 4: CLT plate optimized with both gaps and changing layer thickness.

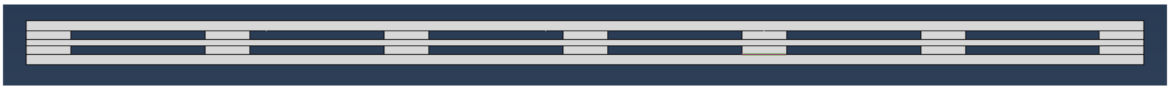

Figure 5.5: Visualization of configuration 4 in Abaqus

5.2.2 Geometric information

To expand on the visualization of the configurations in subsection 5.2, table 5.1 compiles some relevant general information. While the layer thickness for the configurations are compiled in table 5.2.

Table 5.1: General information of configurations

	Mass(kg)	Volume(m^3)	Length(m)	Width(m)
Configuration 1	840	2	5	2
Configuration 2	598.08	1.424	5	2
Configuration 3	735	1.75	5	2
Configuration 4	577.08	1.374	5	2

Table 5.2: Layer thicknesses of configurations in mm

	Configuration 1	Configuration 2	Configuration 3	Configuration 4
Layer 1	40	40	50	45
Layer 2	40	40	20	40
Layer 3	40	40	35	25
Layer 4	40	40	20	40
Layer 5	40	40	50	45
Total	200	200	175	195

Furthermore, table 5.3 compiles information related to the gaps. Here, the "reduction factor" have been determined according to equation (2.3) and the "reduced volume" is a measure of how much the volume has been reduced for the specific CLT plate due to the introduction of gaps.

Table 5.3: Geometric information regarding gaps

	Gap size (m)	Reduction factor, Ω (-)	Reduced volume(%)
Configuration 1	0	1	0
Configuration 2	0.6 x 0.04	0.28	28.8
Configuration 3	0	1	0
Configuration 4	0.6 x 0.04	0.28	29.5

5.3 Mesh convergence study, Abaqus

In order to achieve a mesh size which is both time efficient and deliver accurate results, a mesh convergence study was done for the full 3D model, see figure 5.6, and two loading cases for the RVE-models, see figure 5.7 and figure 5.8.

When choosing the elements sizes, creating a symmetric mesh and having relevant data points in the figure to easily see when convergence occur was taken into consideration. As previously mentioned, mesh element type C3D8 was used.

By observing for what element number the results converge, that specific element size was then chosen to be used in further analysis. For the full 3D models, this was an element size of 0.01 m, while for the RVE-models, this was an element size of 0.005 m. To further expand on why the element size is important, the following data are presented in table 5.4.

Full 3D model

Table 5.4: Mesh convergence study data

Element size (m)	Number of elements	Maximum stress (Pa)	Increase (%)
0.01	200000	2777000	0.5
0.00125	90000	2763000	1.2
0.02	25000	2729000	5.8
0.04	3750	2572000	-

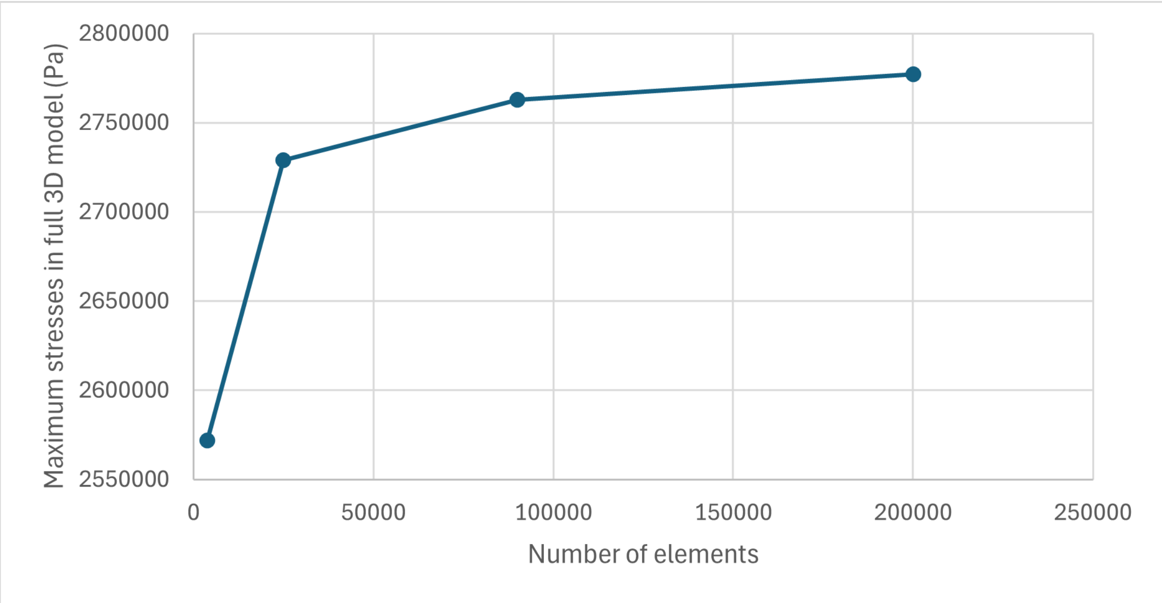

Figure 5.6: Mesh convergence study for full 3D model, configuration 1, uniform load

RVE-model

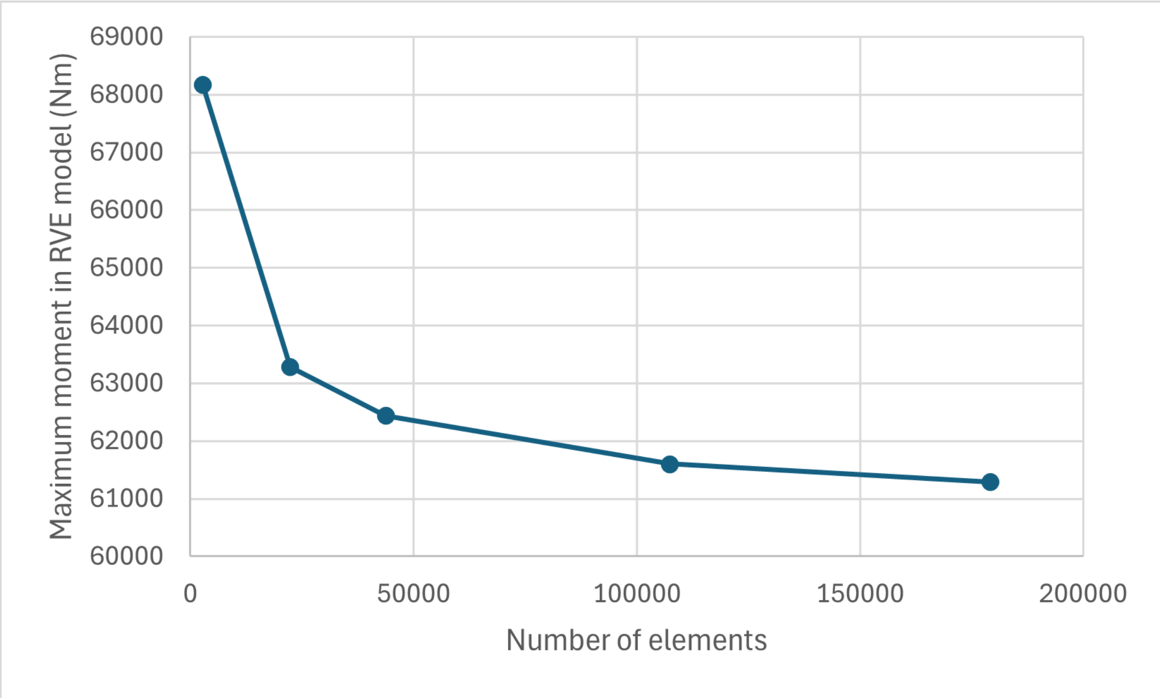

Figure 5.7: Mesh convergence study for RVE model, configuration 2, twist

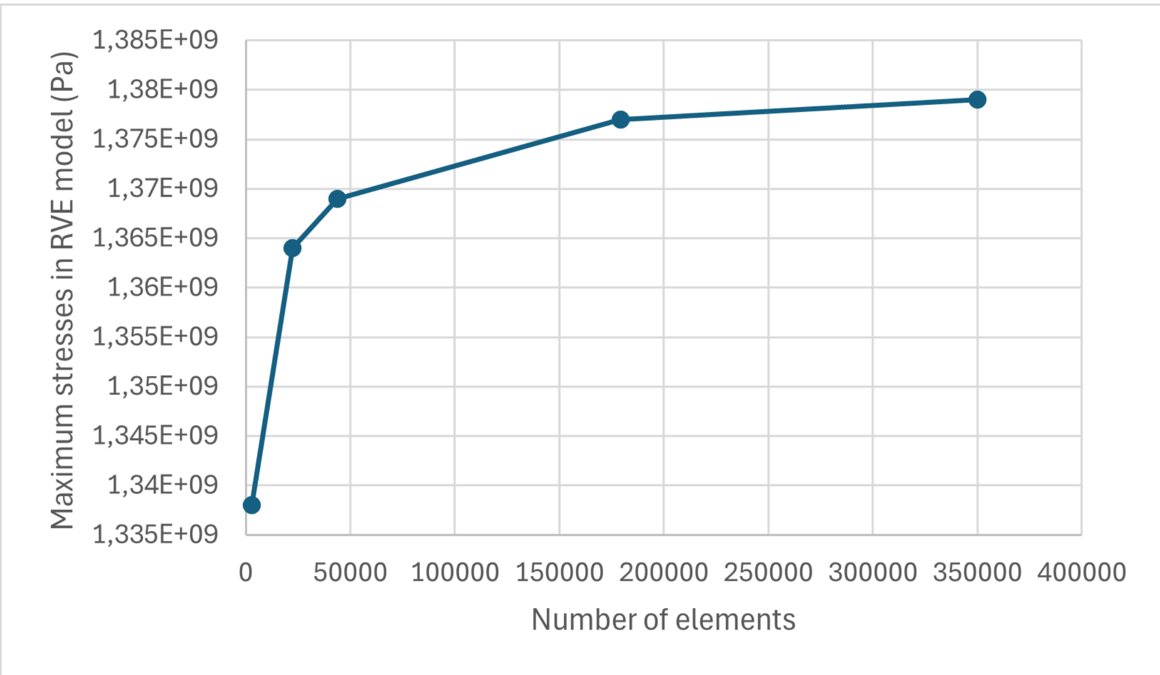

Figure 5.8: Mesh convergence study for RVE model, configuration 2, bending

5.4 Stiffness matrix

In this section, the resulting stiffness matrices from the methods using a stiffness matrix to describe its structural behavior, are compiled. For how the stiffness matrix is created for the method of using a fictitious shell in FEM-design, by homogenization through RVE-models in Abaqus, see section 3.4. While the stiffness matrix used for the method of using a preexisting CLT timber shell in FEM-design, is described in subsection 3.3.1. In regards to units for the specific stiffness parameters, see subsection 3.2.

5.4.1 Configuration 1

Homogenization through RVE-models in Abaqus

$$D_1 = \begin{bmatrix} 5970 & 0 & 0 & 0 & 0 & 0 & 0 & 0 \\ 0 & 1533 & 0 & 0 & 0 & 0 & 0 & 0 \\ 0 & 0 & 162 & 0 & 0 & 0 & 0 & 0 \\ 0 & 0 & 0 & 14765 & 0 & 0 & 0 & 0 \\ 0 & 0 & 0 & 0 & 7977 & 0 & 0 & 0 \\ 0 & 0 & 0 & 0 & 0 & 1370296 & 0 & 0 \\ 0 & 0 & 0 & 0 & 0 & 0 & 869249 & 0 \\ 0 & 0 & 0 & 0 & 0 & 0 & 0 & 111531 \end{bmatrix} \tag{5.2}$$

Stiffness parameter reductions in FEM-design

$$D_1 = \begin{bmatrix} 5808 & 0 & 0 & 0 & 0 & 0 & 0 & 0 \\ 0 & 1525 & 0 & 0 & 0 & 0 & 0 & 0 \\ 0 & 0 & 276 & 0 & 0 & 0 & 0 & 0 \\ 0 & 0 & 0 & 15952 & 0 & 0 & 0 & 0 \\ 0 & 0 & 0 & 0 & 8844 & 0 & 0 & 0 \\ 0 & 0 & 0 & 0 & 0 & 1320000 & 0 & 0 \\ 0 & 0 & 0 & 0 & 0 & 0 & 880000 & 0 \\ 0 & 0 & 0 & 0 & 0 & 0 & 0 & 92460 \end{bmatrix} \tag{5.3}$$

As seen in matrix (5.2) and (5.3), the resulting stiffness values are relatively similar when comparing the two methods for configuration 1.

5.4.2 Configuration 2

Homogenization through RVE-models in Abaqus

$$D_2 = \begin{bmatrix} 5812 & 0 & 0 & 0 & 0 & 0 & 0 & 0 \\ 0 & 405 & 0 & 0 & 0 & 0 & 0 & 0 \\ 0 & 0 & 69 & 0 & 0 & 0 & 0 & 0 \\ 0 & 0 & 0 & 2288 & 0 & 0 & 0 & 0 \\ 0 & 0 & 0 & 0 & 2571 & 0 & 0 & 0 \\ 0 & 0 & 0 & 0 & 0 & 1326468 & 0 & 0 \\ 0 & 0 & 0 & 0 & 0 & 0 & 228135 & 0 \\ 0 & 0 & 0 & 0 & 0 & 0 & 0 & 33104 \end{bmatrix} \tag{5.4}$$

Stiffness parameter reductions in FEM-design

$$D_2 = \begin{bmatrix} 5808 & 0 & 0 & 0 & 0 & 0 & 0 & 0 \\ 0 & 427 & 0 & 0 & 0 & 0 & 0 & 0 \\ 0 & 0 & 235 & 0 & 0 & 0 & 0 & 0 \\ 0 & 0 & 0 & 4677 & 0 & 0 & 0 & 0 \\ 0 & 0 & 0 & 0 & 7695 & 0 & 0 & 0 \\ 0 & 0 & 0 & 0 & 0 & 1320000 & 0 & 0 \\ 0 & 0 & 0 & 0 & 0 & 0 & 246400 & 0 \\ 0 & 0 & 0 & 0 & 0 & 0 & 0 & 65821 \end{bmatrix} \tag{5.5}$$

To showcase how the introduction of gaps affect the values of the stiffness matrix, a comparison is made between matrix (5.2) and matrix (5.4) in table 5.5. The stiffness parameters which are to be compared are the bending stiffness in the strong direction, D_{11}, and the out of plane shear stiffness, D_{44}, in the strong direction, see subsection 3.2. The reason for comparing these two specifically is that they have the greatest effect on the results of the specific design case preconditions, being a plate spanning one way, see subsection 5.1.

Table 5.5: Comparison between matrix 5.2 and matrix 5.4.

	Configuration 1	Configuration 2	Reduction (%)
Bending stiffness (kNm/m)	5970	5812	2.6
Shear stiffness (kN/m)	14765	2288	85.5

5.4.3 Configuration 3

Homogenization through RVE-models in Abaqus

$$D_3 = \begin{bmatrix} 4696 & 0 & 0 & 0 & 0 & 0 & 0 & 0 \\ 0 & 362 & 0 & 0 & 0 & 0 & 0 & 0 \\ 0 & 0 & 191 & 0 & 0 & 0 & 0 & 0 \\ 0 & 0 & 0 & 18222 & 0 & 0 & 0 & 0 \\ 0 & 0 & 0 & 0 & 4093 & 0 & 0 & 0 \\ 0 & 0 & 0 & 0 & 0 & 1538697 & 0 & 0 \\ 0 & 0 & 0 & 0 & 0 & 0 & 440851 & 0 \\ 0 & 0 & 0 & 0 & 0 & 0 & 0 & 99810 \end{bmatrix} \tag{5.6}$$

Stiffness parameter reductions in FEM-design

$$D_3 = \begin{bmatrix} 4565 & 0 & 0 & 0 & 0 & 0 & 0 & 0 \\ 0 & 347 & 0 & 0 & 0 & 0 & 0 & 0 \\ 0 & 0 & 185 & 0 & 0 & 0 & 0 & 0 \\ 0 & 0 & 0 & 19322 & 0 & 0 & 0 & 0 \\ 0 & 0 & 0 & 0 & 4560 & 0 & 0 & 0 \\ 0 & 0 & 0 & 0 & 0 & 1485000 & 0 & 0 \\ 0 & 0 & 0 & 0 & 0 & 0 & 440000 & 0 \\ 0 & 0 & 0 & 0 & 0 & 0 & 0 & 80902 \end{bmatrix} \tag{5.7}$$

As seen in matrix (5.6) and (5.7), the resulting stiffness values are relatively similar when comparing the two methods for configuration 3.

5.4.4 Configuration 4

Homogenization through RVE-models in Abaqus

$$D_4 = \begin{bmatrix} 5758 & 0 & 0 & 0 & 0 & 0 & 0 & 0 \\ 0 & 279 & 0 & 0 & 0 & 0 & 0 & 0 \\ 0 & 0 & 56 & 0 & 0 & 0 & 0 & 0 \\ 0 & 0 & 0 & 1948 & 0 & 0 & 0 & 0 \\ 0 & 0 & 0 & 0 & 2591 & 0 & 0 & 0 \\ 0 & 0 & 0 & 0 & 0 & 1271024 & 0 & 0 \\ 0 & 0 & 0 & 0 & 0 & 0 & 227268 & 0 \\ 0 & 0 & 0 & 0 & 0 & 0 & 0 & 28140 \end{bmatrix} \tag{5.8}$$

Stiffness parameter reductions in FEM-design

$$D_4 = \begin{bmatrix} 5750 & 0 & 0 & 0 & 0 & 0 & 0 & 0 \\ 0 & 293 & 0 & 0 & 0 & 0 & 0 & 0 \\ 0 & 0 & 227 & 0 & 0 & 0 & 0 & 0 \\ 0 & 0 & 0 & 4135 & 0 & 0 & 0 & 0 \\ 0 & 0 & 0 & 0 & 7813 & 0 & 0 & 0 \\ 0 & 0 & 0 & 0 & 0 & 1265000 & 0 & 0 \\ 0 & 0 & 0 & 0 & 0 & 0 & 246400 & 0 \\ 0 & 0 & 0 & 0 & 0 & 0 & 0 & 63509 \end{bmatrix} \tag{5.9}$$

To compare how the two different methods take the gaps into consideration, it is observed that the two methods result in differing stiffness values for the following four stiffness parameters, see subsection 3.2.

- Torsional stiffness, D_{33}.
- Out of plane shear stiffness, D_{44} and D_{55}.
- In plane shear stiffness, D_{88}

5.5 Compilation of checks according to ULS and SLS

In table 5.6, table 5.7 and table 5.8, the utilization rate for the ultimate limit state checks are compiled. The utilization rate for the three different checks are found in their respective subsections in section 4 and is calculated by (4.5), (4.10) and (4.14) respectively.

As a reminder, FEM-design, fictitious shell was made by creation of a stiffness matrix through RVE-models in Abaqus. While FEM-design, timber shell utilizes a stiffness matrix which is created by the program itself through reduction of parameters.

The frequency check has been divided into two separate cases, unloaded frequency and loaded frequency. Where the loaded frequency utilizes the m according to 4.2.2, which included the contribution of the loads acting on the plate. The unloaded frequency is excluding the contribution of these loads and only utilizes the self weight to give further knowledge of the plates performance.

5.5.1 Bending moment, ultimate limit state

For the resulting utilization rate for the bending moment check, it is observed that the gamma method gives a higher result compared to the other methods for the regular CLT. While the results of FEM-design results in very similar results to the shear analogy method and Timoshenko theory. Furthermore, the utilization rate for the CLT configurations with gaps are higher for the method using a 3D Abaqus model compared to the other methods.

Table 5.6: Utilization rate bending moment check

Bending moment check	Conf 1	Conf 2	Conf 3	Conf 4
Gamma method	26.7 %	25.9 %	28.6 %	25.9 %
Timoshenko theory	26.1 %	23.9 %	28.0 %	23.4 %
Shear analogy method	26.1 %	23.9 %	28.0 %	23.4 %
FEM-design, timber shell	26.1 %	23.9%	28.0 %	23.4 %
FEM-design, fictitious shell	25.4 %	23.9 %	28.0 %	23.3 %
Abaqus	26.1%	34.5 %	28.0 %	36.3 %

5.5.2 Longitudinal shear, ultimate limit state

For the longitudinal shear checks in table 5.7, the results vary in the same way as shown for the bending moment check in the previous subsection. It is also observed that the utilization rate in general is much lower for the longitudinal shear check compared to the bending moment check.

Table 5.7: Utilization rate of longitudinal shear check.

Longitudinal shear check	Conf 1	Conf 2	Conf 3	Conf 4
Gamma method	4.89 %	4.52 %	6.06 %	4.87 %
Timoshenko theory	4.87 %	4.46 %	5.76 %	4.54 %
Shear analogy method	4.87 %	4.46 %	5.76 %	4.54 %
FEM-design, timber shell	4.90 %	4.50 %	5.80 %	4.54 %
FEM-design, fictitious shell	4.74 %	4.46 %	5.60 %	4.54 %
Abaqus	5.09 %	16.6 %	5.74 %	17.9 %

5.5.3 Rolling shear, ultimate limit state

In table 5.8, it is observed that the utilization rate for the rolling shear is much higher than for the longitudinal shear check, and that the 3D model in Abaqus results in a significantly higher utilization rate for rolling shear in the configurations with gaps. It is important to note that the rolling shear results for all methods except Abaqus are given by the conventional formulas for standard CLT which might heavily underestimate the affect of the gaps.

Table 5.8: Utilization rate of rolling shear check

Rolling shear check	Conf 1	Conf 2	Conf 3	Conf 4
Gamma method	22.8 %	20.7 %	27.3 %	21.8 %
Timoshenko theory	22.9 %	21.0 %	27.4 %	22.2 %
Shear analogy method	22.9 %	21.0 %	27.4 %	22.2 %
FEM-design, timber module	22.9 %	21.0 %	27.4 %	22.2 %
FEM-design, fictitious shell	22.3 %	21.0 %	26.7 %	22.2 %
Abaqus	22.7 %	64.8 %	26.7 %	65.3 %

5.5.4 Unloaded frequency, serviceability limit state

By observing the frequency, it is shown that the results for the Timoshenko theory and the shear analogy method are deviant compared to the other methods which show a similar result for the regular CLT configuration. For the configurations with gaps, a more varying result is displayed between methods. It is also shown that the introduction of gaps results in a higher frequency. However, for fictitious shell in FEM-design and the 3D Abaqus model, the frequency is lowered with the introduction of gaps.

Table 5.9: Unloaded frequency, 8 Hz limit

Unloaded frequency check	Conf 1	Conf 2	Conf 3	Conf 4
Gamma method	15.5 Hz	16.1 Hz	15.1 Hz	16.0 Hz
Timoshenko theory	16.5 Hz	19.58 Hz	15.7 Hz	19.8 Hz
Shear analogy method	16.5 Hz	19.58 Hz	15.7 Hz	19.8 Hz
FEM-design, timber shell	15.4 Hz	16.0 Hz	15.0 Hz	15.9 Hz
FEM-design, fictitious shell	15.6 Hz	13.8 Hz	15.1 Hz	13.5 Hz
Abaqus	15.5 Hz	14.4 Hz	15.0 Hz	14.2 Hz

5.5.5 Loaded frequency, serviceability limit state

Again, by observing the frequency, it is shown that the results for the Timoshenko theory and the shear analogy method are deviant compared to the other methods which show a similar result for the regular CLT configuration. For the configurations with gaps, a more varying result is again displayed between methods. However, it is observed that the introduction of gaps for the gamma method, results in a lowered loaded frequency, instead of an increase as for the unloaded frequency. Furthermore, the configurations with gaps fail the design check for some of the methods, as the frequency is below the limit of 8. These methods being fictitious shell in FEM-design and Abaqus for configuration 2 and timber shell in FEM-design, fictitious shell in FEM-design and Abaqus for configuration 4.

Table 5.10: Loaded frequency, 8 Hz limit

Loaded frequency check	Conf 1	Conf 2	Conf 3	Conf 4
Gamma method	8.87 Hz	8.17 Hz	8.22 Hz	8.02 Hz
Timoshenko theory	9.44 Hz	9.92 Hz	8.55 Hz	9.92 Hz
Shear analogy method	9.44 Hz	9.92 Hz	8.55 Hz	9.92 Hz
FEM-design, timber shell	8.83 Hz	8.12 Hz	8.17 Hz	7.96 Hz
FEM-design, fictitious shell	8.89 Hz	7.01 Hz	8.26 Hz	6.74 Hz
Abaqus	8.86 Hz	7.30 Hz	8.18 Hz	7.12 Hz

5.5.6 Deflection, serviceability limit state

The configurations with gaps result in a higher utilization rate for the deflection according to all methods. However, fictitious shell in FEM-design and the 3D Abaqus model display a significantly higher utilization rate. For the regular CLT configurations, all the methods give a similar result.

Table 5.11: Utilization rate of final deflection

Deflection	Conf 1	Conf 2	Conf 3	Conf 4
Gamma method	57.8 %	69.8 %	68.0 %	72.8 %
Timoshenko theory	58.1 %	70.0 %	68.6 %	72.9 %
Shear analogy method	57.7 %	71.1 %	68.6 %	74.4 %
FEM-design, timber shell	58.1 %	70.0 %	68.6 %	73.0 %
FEM-design, fictitious shell	57.3 %	92.6 %	67.2 %	101 %
Abaqus	57.6 %	88.7 %	68.4 %	93.1 %

5.5.7 Point load criterion, serviceability limit state

For the point load criterion, the analytical methods result in the following performance levels. The gamma method results in the same level for all configurations, while the level varies for Timoshenko theory and the shear analogy method.

Table 5.12: Performance class for unit point deflection

Point load criterion	Conf 1	Conf 2	Conf 3	Conf 4
Gamma method	III	III	III	III
Timoshenko theory	I	I	III	I
Shear analogy method	I	I	III	I
FEM-design, timber shell	-	-	-	-
FEM-design, fictitious shell	-	-	-	-
Abaqus	-	-	-	-

5.5.8 Velocity response, serviceability limit state

For the velocity response, the analytical methods resulted in the following performance level.

Table 5.13: Performance class velocity response

Velocity response	Conf 1	Conf 2	Conf 3	Conf 4
Gamma method	V	V	V	V
Timoshenko theory	IV	V	V	V
Shear analogy method	IV	V	V	V
FEM-design, timber shell	-	-	-	-
FEM-design, fictitious shell	-	-	-	-
Abaqus	-	-	-	-

5.6 Material savings

5.6.1 According to analytical methods

When the material savings achieved according to the analytical methods are observed, the most reasonable reference for comparison would be the optimized regular CLT. The reason being the material savings achieved with configuration 1 as reference would be missleading. Therefore, the material savings achieved for the configurations with gaps are presented in table 5.14 with configuration 3 as a reference.

Table 5.14: Material saving of configuration 2 and configuration 4 with configuration 3 as reference

Material saving	Unit	Value
Configuration 2	%	18.6
Configuration 4	%	21.5

5.6.2 According to 3D FE-analysis

As it is assumed that the results from the 3D models made in Abaqus are the best representation of reality, an optimized configuration was developed by introducing gaps and changing the layer thickness. This is done to investigate and determine a more realistic material savings percentage compared to the results in subsection 5.6.1. As the loaded frequency has shown to be the governing parameter when optimizing the other CLT configurations, this configuration was also optimized with the goal of the frequency reaching a value higher than 8 Hz. The geometric information is compiled in table 5.15 and the configuration is visualized in figure 5.9:

Table 5.15: Geometric information of configuration 5

Configuration 5	Unit	Value
Mass	kg	661.08
Volume	m^3	1.574
Reduction factor	(-)	0.28
Layer thicknesses	mm	45, 40, 45, 40, 45
Material savings	%	10

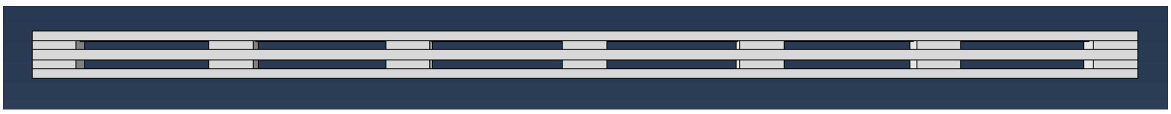

Figure 5.9: Visualization of configuration 5 in Abaqus

6 Concluding remarks

6.1 Discussion and conclusion

For comparison of the stiffness matrix for the different configurations with one another, configuration 1 and configuration 2 are suitable options, as they have the same preconditions except for the gaps. It is concluded that the gaps significantly reduce the out of plane shear stiffness, in plane shear stiffness and the torsional stiffness. However, the bending stiffness and the membrane stiffness for the strong direction remain relatively unchanged, while their respective stiffness in the weak direction is proportionally reduced to the reduction of the volume in the cross layer. Another relevant comparison is made between the stiffness matrix for the two different methods used, where it is concluded that the stiffness values are very similar for the regular CLT. However, the method of stiffness parameter reduction in FEM-design overestimates and fails to fully take the reduction in torsional stiffness, in plane shear stiffness and out of plane shear stiffness due to gaps into consideration.

Upon examining the results in the ultimate limit state for the analytical methods, the configurations with gaps give a lower utilization rate compared to the standard configurations. This result can be explained by the design load being smaller as the contribution of the self weight is less. Furthermore, the FEM-design methods are aligned with the results of the analytical methods, while the 3D model in Abaqus instead display a higher utilization rate for the configurations with gaps. The reason being the stress increases around the gaps is taken into consideration in the 3D model. Regarding the configurations without gaps, all the different methods gave a similar result. It is therefore concluded that the analytical methods cannot be used to properly predict the design stresses in CLT design with the introduction of gaps. It is also concluded that the increase of design stresses due to gaps is much higher for shear compared to bending.

As the analytical methods are compared to each other when looking at a specific configuration, it is observed that the shear analogy method and Timoshenko theory give the exact same results. This is consistent throughout the design checks in both the ultimate limit state and the serviceability state, except for deformation. The reason being that the usage of the methods results in the same bending stiffness, while the shear stiffness differs, which is only applied in the equations calculating the deformation. As it is also observed that the gamma method generally results in the closest results to the 3D model, as it is able to take the reduced stiffness into account in the gamma factor. The results with FEM-designs timber shell again closely align with the shear analogy method and Timoshenko theory.

In regard to the deflection, all the methods gave a similar result except for the 3D model done in Abaqus and FEM-design using a fictitious shell. The remaining methods fail to take the shear stiffness properly into account, even though the reduction factor is used on the stiffness parameters in calculations. The conclusion being that these methods cannot be used for deflection calculations. However, as it is known that the shear reduction is not proportional to the volume reduction, as the bending stiffness is, the possibility of determining a separate shear reduction factor exists, giving a more realistic result for the deflection when using the analytical methods, see section 6.3.

Because the analytical methods cannot properly predict the behavior of the "Gap CLT", it is concluded that the material savings results according to these methods are less reliable. This conclusion is based on that the observed design parameter, frequency, for these methods was optimized to the highest possible utilization rate. While its finite element method counterpart for the configurations with gaps resulted in a lower than acceptable frequency. As the frequency is the deciding design parameter, optimization in Abaqus was done for a more realistic prediction how much material savings is possible. It was concluded that at least 10 % is possible for this specific design case, a result that may vary depending on the preconditions of the specific design case.

6.2 Sources of error

Possible sources of errors that could have affected the results in the project is the human error factor of simple miscalculations. This mainly applies to the calculations performed in excel for the analytical methods.

There is also the possibility of the usage of the wrong boundary conditions while modeling the RVE-models or the full 3D plate in Abaqus. This could possibly lead to a model being created which is not truly comparable to the conditions of the plate being simply supported, or for the RVE-models, not being a good representation of a symmetry cut in a random position of the CLT plate.

For the RVE-models, the choice of coupling could be a source of error. The reason for this is that the RVE-model with distributed coupling, resulted in a asymmetric deformation pattern for the out of plane shear RVE-model, as shown in figure 6.1. A RVE-model with the same boundary conditions but with kinematic coupling resulted in a more realistic deformation pattern as shown in figure 6.2 However, it resulted in a much more unrealistic stiffness result, an increase by a factor of 4. Therefore, it was determined that the RVE-model with distributed coupling would be the one which is used, even though its asymmetric deformation pattern. The reason for the deformation pattern being unrealistic is that it does not perfectly represent a symmetry, mainly due to the deformation of the central longitudinal layer. This is relevant for both in and out of plane shear.

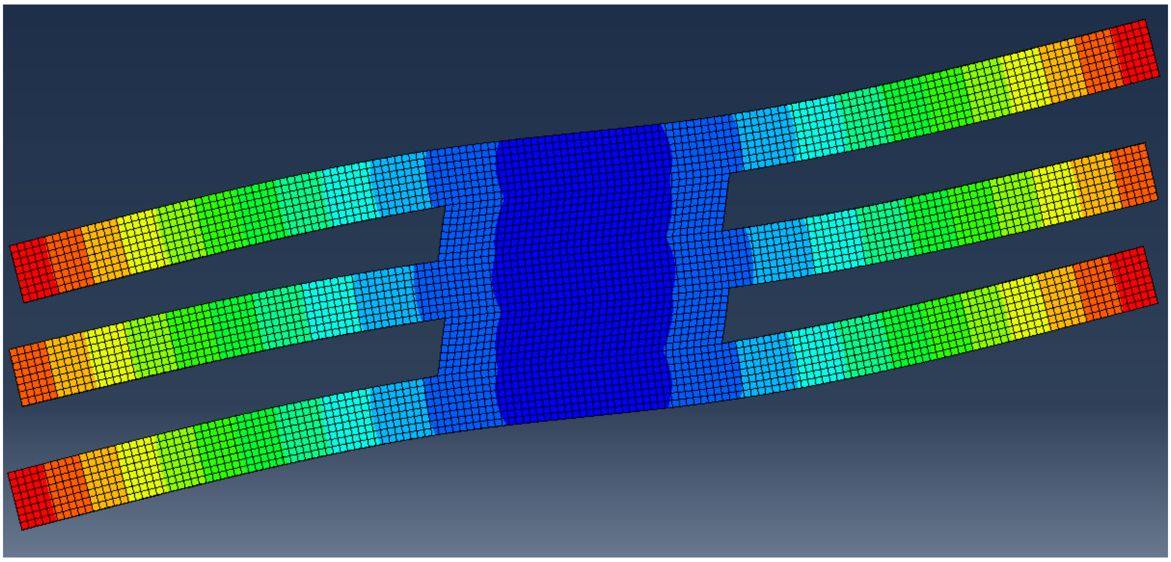

Figure 6.1: Out of plane shear with distributed coupling

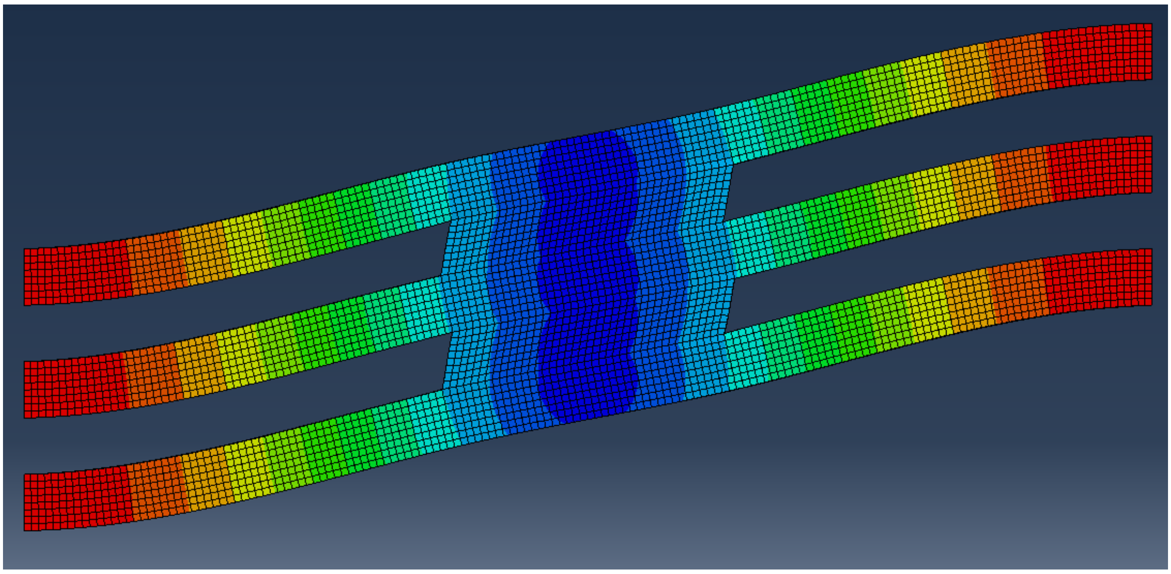

Figure 6.2: Out of plane shear with kinematic coupling

However, for the two types of coupling, bending did not result in a differing deformation pattern, see figure 6.3 and figure 6.4:

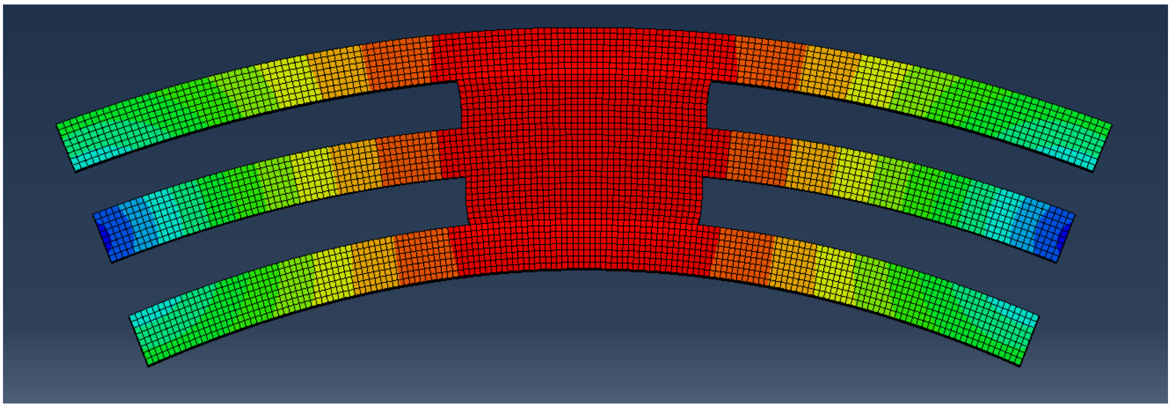

Figure 6.3: Bending in strong direction with distributed coupling

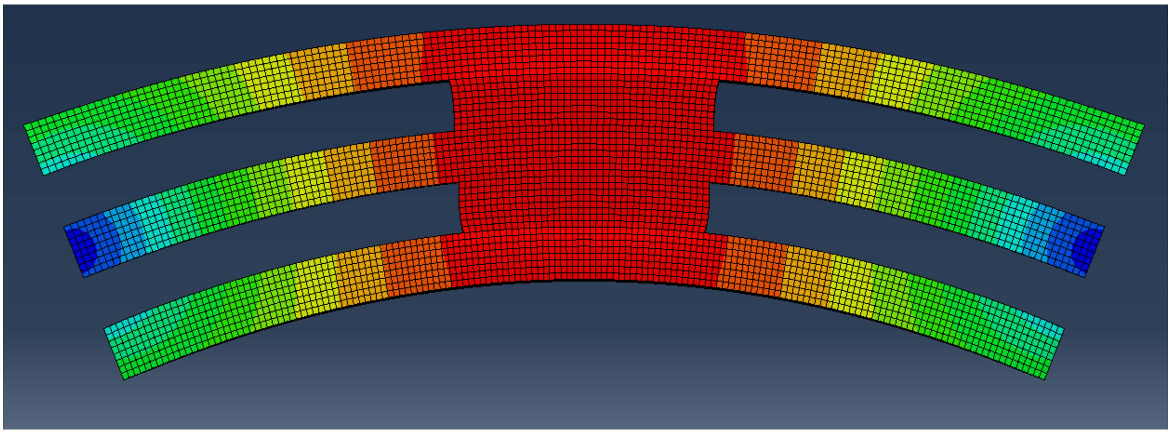

Figure 6.4: Bending in strong direction with kinematic coupling

6.3 Future work

A suitable next step in the progress of "gap CLT" as a product is for future work to determine a possible solution for the analytical methods to be able to consider the increased stresses due to gaps. For beams with holes, there is a factor denoted κ_{corner} which takes this increased stress into account, although the gaps considered with this factor are much smaller than the ones considered in this project. A similar approach would benefit the design of "gap CLT" in the ultimate limit state.

In regards to the rolling shear, it was decided that the conventional formula was to be used in the ultimate limit state. However, with the introduction of the gaps, the equilibrium in which this formula is based upon is no longer fulfilled. Although it is possible to derive a new formula with beam theory.

Another thing that could be determined in future work is in regards to the shear reduction factor as mentioned in the deflection part of the discussion in section 6.1. A possible way to determine this factor is by creating a RVE-model in Abaqus for a CLT plate with gaps and one without gaps to get a reference value. By comparing the stiffnesses of these models, a stiffness reduction factor is achieved, which in turn can be applied to the stiffness parameters in deflection calculations and give similar results to the 3D finite element analysis model. The development of a formula or table of shear reduction factors for different configurations of gaps would therefore aid the analytical methods.

Future work which would build on this project is to further examine the possibilities and limitations of "gap CLT" by exploring similar questions as this project. However, expanding on it by for example examining 7 layer configurations and examine the effect of the plate spanning different lengths. Another case worth examining is the effect of having the plate span in 2 directions, along with this, gaps in both directions could also be examined. Possible future work could also examine the excluded parts mentioned in "Limitation", see section 1.4.

To showcase why the future work is important for "Gap CLT", the difference in behavior can be illustrated by comparing the following two models from Abaqus. Shown in figure 6.5 and figure 6.6, are view cuts of configuration 1 and configuration 2. Here, the differences in bending stress distribution and concentration is visible, as visualized by the darker shades of red and blue. It is worth to notice that the regular CLT model follows the principle of the bending stresses being the highest at the middle of the span, however, this is shown to not be the case in the "Gap CLT" model. The difference in the deflection pattern due to the lack of stiffness at the location of the gaps is also visible, as the pattern can be described as irregular.

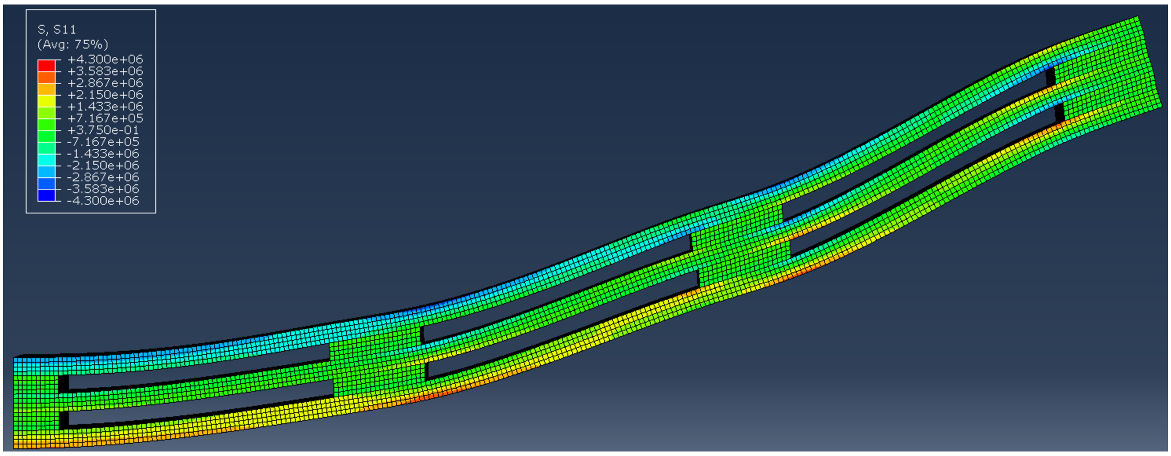

Figure 6.5: Bending stresses and deflection for a "Gap CLT" configuration

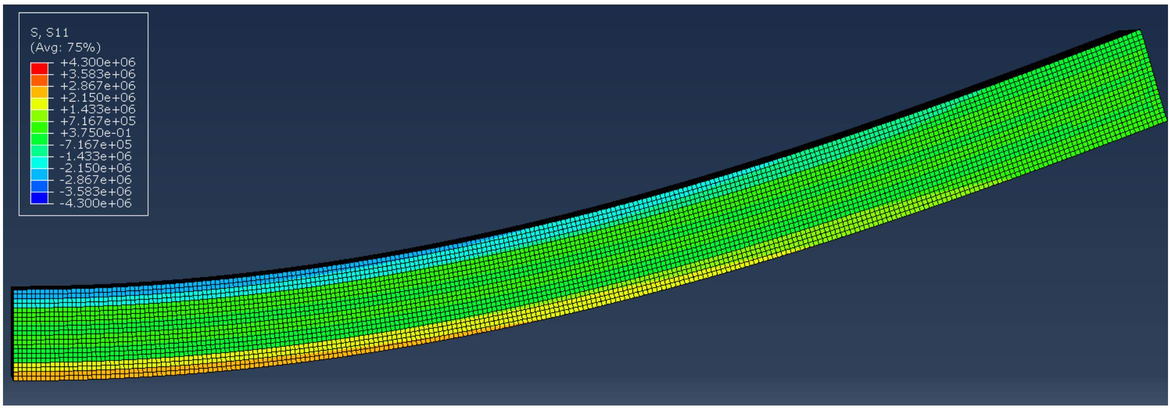

Figure 6.6: Bending stresses and deflection for a regular CLT configuration

Bibliography

[1] H. J. Blass and C. Sandhaas. *Timber engineering - Principles for design.* KIT Scientific publishing, (2017).

[2] G. Ravenshorst. “Species independent strength grading of structural timber”. PhD thesis. Technische Universiteit Delft, (2015).

[3] A. Gustafson et al. *”KL-trähandboken, Fakta och projektering av KL-träkonstruktioner”*. Svenskt trä, (2017).

[4] T. Isaksson and A. Mårtensson. *”Byggkonstruktion - Regel och formelsamling”*. Studentlitteratur, (2019).

[5] M. Wallner-Novak et al. *”Cross-Laminated Timber Structural design”*. pro:Holz, (2014).

[6] L. Franzoni et al. “Elastic behavior of Cross Laminated Timber and timber panels with regular gaps: Thick-plate modeling and experimental validation”. In: *Engineering Structures* 141 (2017).

[7] A. Moberg and L. Xiao. “Next generation CLT”. MA thesis. Chalmers University of technology, 2022.

[8] G. Demissie. “Understanding analyctical methods of clt: shear analogy, gamma, extended gamma, and timoshenko beam theory methods”. In: *SPEC Toolbox* (2024).

[9] M. Wallner-Novak et al. *”Cross-Laminated Timber Structural design Volume 2”*. pro:Holz, (2018).

[10] M. Tahmasebi and H. Kurzawinska. “Performance optimization of CLT”. MA thesis. Chalmers University of technology, (2023).

[11] E. Karacabeyli and S. Gagnon. *Canadian CLT Handbook.* FPinnovations, (2019).

[12] *”Abaqus/CAE - User’s guide”*. Dassault systemes, (2016).

[13] *”User manual, FEM-Design”*. Strusoft, (2010).

[14] J. Wetterholt. “Modelling cross-laminated timber floor in dynamic analysis-Eigenfrequency prediction”. MA thesis. Lunds teknika högskola, 2019.

[15] T. Arbogast. “Composite materials and homogenization”. In: *Encyclopedia of applied and computational mathematics* (2015).

[16] M. A. Kaddaha et al. “Homogenization method to calculate the stiffness matrix of laminated composites”. In: *Eng* (2021).

[17] *Eurocode 5 – Design of timber structures – Part 1-1: General rules and rules for building.* SS-EN 1995-1-1 :2025. Swedish Standards Institution, 2025.